Cost-Reliability Tradeoff in Licensed and Unlicensed Spectra Interoperable Networks With Guaranteed User Data Rate Requirements

Hao Song, *Student Member, IEEE*, Xuming Fang, *Senior Member, IEEE*, and Cheng-Xiang Wang, *Fellow, IEEE*

***Abstract*— Unlicensed spectra access holds the promise of alleviating licensed spectra scarcity and providing super high-rate mobile data services, which has been viewed as one of the key technologies of fifth generation (5G) cellular networks. In this paper, we first design a framework for 5G licensed and unlicensed spectra interoperable networks based on the cloud radio access network technology and the control/data decoupled architecture. Then, we investigate network-level cost-reliability tradeoff from two aspects. First, we study a fundamental tradeoff between the cost and the reliability by minimizing cost for a given reliability level. Second, we define a quality of experience efficiency utility as the complementary measure to characterize the cost and the reliability, offering an inherent tradeoff between them. Moreover, an interference power estimation method is proposed to more accurately estimate channel states to guarantee resource allocation effectiveness. Finally, we conduct extensive simulation study and demonstrate the effectiveness of the interference power estimation method.**

***Index Terms*— C-RAN, control/data decoupling, joint licensed/unlicensed resource allocation, cost-reliability tradeoff, QoE efficiency.**

I. Introduction

ACCORDING to the study and forecast conducted by CISCO [1], mobile data traffic has been witnessed tremendous growth and will increase nearly eight-fold with the compound annual growth rate (CAGR) of 53% between 2015 and 2020. However, only relying on spectral efficiency improvement and network densification, current widely used network capacity enhancement strategies, will not catch up with this exponential growth. Therefore, spectrum extension, as the most straight-forward solution, has attracted more and more attention recently. Unfortunately, as a scarce and costly resource, it is hard for operators to obtain more licensed spectra. Using unlicensed spectra, such as industrial, scientific and medical (ISM), and unlicensed national information infrastructure (UNII) bands, holds the promise of aiding limited licensed spectra. Currently, LTE systems have been encouraged to utilize unlicensed spectra, such as LTE-unlicensed (LTE-U) and licensed-assisted access (LAA) systems [2], and the corresponding enabling technologies have been widely studied. For example, Khawer *et al.* [3] research smallcell interference mitigation strategy for LTE-U systems. The energy efficiency optimization for LAA systems is studied in [4]. Besides low frequency unlicensed bands, ultra-wideband mmWave bands have been opened up for unlicensed use, such as 24-24.25GHz, 28-30GHz and 57-64GHz bands [5]. Hence, unlicensed spectra access has been viewed as one of the key technologies for 5G mobile networks, which are highly probable to access limited licensed spectra and ultra-wideband unlicensed spectra simultaneously [6], [7].

However, unlicensed spectra are usually distributed over high frequency bands with high path loss, the transmission on which should strictly comply with the power limitation ruled by government. To keep pace with those, dense microcell networks are needed for unlicensed spectra coverage [3]. Conversely, licensed spectra are always distributed over low frequency bands with low path loss, and high power is allowed to be used to transmit signals. These can facilitate macrocell coverage of licensed spectra to provide wide-range and reliable transmission for broadcast and signaling, and reduce the frequency of handoff [6], [8]. Therefore, 5G licensed and unlicensed interoperable networks could well be deployed with heterogeneous network architecture. However, in such an architecture, the issues, such as high system complexity, complicated resource management, etc., need to be addressed to guarantee feasibility. Hence, we design a 5G licensed and unlicensed interoperable network based on the C-RAN technology, which is a promising architecture of 5G mobile networks [9].

In such a network, users need to communicate on licensed and unlicensed spectra, simultaneously. It is noteworthy that huge differences exist between licensed and unlicensed spectra in terms of cost and reliability. To be specific, due to license-free nature, the use of unlicensed spectra would be more economical than licensed spectra. However, due to uncontrollable interference suffered from coexisting wireless

Manuscript received April 29, 2016; revised August 10, 2016; accepted November 6, 2016. Date of publication November 24, 2016; date of current version January 12, 2017. This work was supported in part by the EU FP7 QUICK Project under Grant PIRSESGA-2013-612652, in part by the International S&T Cooperation Program of China under Grant 2014DFA11640, in part by the EU H2020 ITN 5G Wireless Project under Grant 641985, and in part by the EPSRC TOUCAN Project under Grant EP/L020009/1. The work of H. Song and X. Fang was supported in part by the 973 Program of China under Grant 2012CB316100 and in part by NSFC under Grant 61471303, U1501255. *(Corresponding author: Xuming Fang.)*

H. Song and X. Fang are with the Department of Information Science and Technology, Southwest Jiaotong University, Chengdu 611756, China (e-mail: songhao992013@gmail.com; xmfang@swjtu.edu.cn).

C.-X. Wang is with the School of Engineering and Physical Sciences, Institute of Sensors, Signals and Systems, Heriot-Watt University, Edinburgh, EH14 4AS, U.K. (e-mail: cheng-xiang.wang@hw.ac.uk).

Color versions of one or more of the figures in this paper are available online at http://ieeexplore.ieee.org.

Digital Object Identifier 10.1109/JSAC.2016.2633072

0733-8716 © 2016 IEEE. Personal use is permitted, but republication/redistribution requires IEEE permission.
See http://www.ieee.org/publications_standards/publications/rights/index.html for more information.

systems, wireless transmission on unlicensed spectra would be less reliable than that on licensed spectra with exclusive ownership. Accordingly, high transmission reliability always means more licensed spectra usage with high cost, while low cost always brings in low reliability due to more unlicensed spectra utilized. Most studies on network optimization focus on spectral efficiency (SE) and energy efficiency (EE) to enhance system capacity and achieve green communications, respectively [10]– [12]. Unfortunately, jointly enhancing both SE and EE is challenging, because achieving an improvement of one of them always means sacrificing the other [13]. Thus, a fundamental tradeoff between SE and EE has been widely studied. For example, by adjusting the resource allocation, such as power distribution and channel assignment, Haider *et al.* [13], Zhang *et al.* [14], and Xiong *et al.* [15] study the SE-EE tradeoff for mobile femtocell, cognitive radio, and frequency division multiple access (OFDMA) networks, respectively. Additionally, since the economic efficiency (ECE) originally introduced in [16] implicitly considers SE and EE as both metrics reflect revenues and costs of network, it potentially offers a good measure to perform SE-EE tradeoff [17]. By maximizing ECE, Patcharamaneepakorn *et al.* [17] and Ku *et al.* [18] explore the SE-EE tradeoff for generalized spatial modulation and relay-aided cellular networks, respectively. Besides SE-EE tradeoff, recent studies have been extended to multiple types of tradeoffs, in which two different performance metrics are always conflicting with each other, such as energy-delay tradeoff in green cellular networks [19], EE-delay tradeoff in device-to-device communications in underlaying cellular networks [20] and throughput-delay tradeoff in mobile ad hoc networks [21], etc. However, to the best of our knowledge, there is still no work done on cost-reliability tradeoff for licensed and unlicensed interoperable networks.

In this paper, we focus on investigating the cost-reliability tradeoff in licensed and unlicensed interoperable networks by adjusting joint licensed/unlicensed resource allocation strategy, including channel assignment and power distribution. The main objective of resource allocation is to maintain planned system performance, which is carried out based on periodic channel state measurement. However, according to [22] and [23], channel state feedback delay may significantly degrade system performance, particularly in a radio environment with uncontrollable interference. This is because in such a radio environment, measured channel state may significantly differ from actual one at actual transmission time [24]. The gap between them could make resource allocation algorithm unable to reach the planned system performance, namely, poor resource allocation effectiveness. Thus, the inaccuracy of measured channel states is a challenging problem for licensed and unlicensed interoperable networks.

Based on the aforementioned analysis, our main contributions of this paper are summarized as follows:

1) We put forward an interference power estimation method to more accurately estimate channel states to guarantee resource allocation effectiveness.

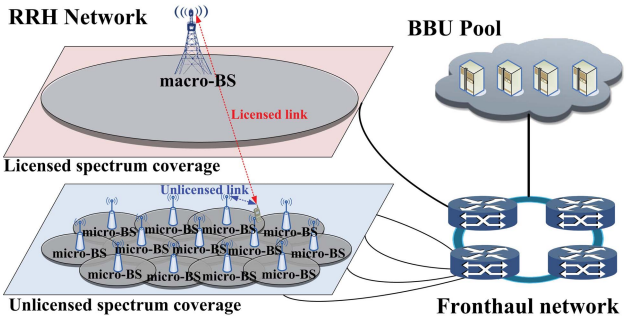

Fig. 1. C-RAN based licensed and unlicensed interoperable networks architecture.

2) We investigate a fundamental cost-reliability tradeoff by solving a cost minimization problem with a given reliability constraint. Then, inspired by SE-EE tradeoff with ECE, we put forward a QoE efficiency utility as a complementary performance measure for cost and reliability to assess an inherent tradeoff between them.

The remainder of this paper is organized as follows. In Section II, we describe the framework and the corresponding system model of C-RAN based licensed and unlicensed interoperable network. Section III presents our proposed interference power estimation method, and defines cost and reliability utilities. In Section IV, we investigate the cost-reliability tradeoff by minimizing cost for a given reliability. Then, a QoE efficiency utility is proposed to study cost-reliability tradeoff in Section V. Simulation studies are carried out in Section VI. Finally, Section VII concludes the paper and outlines future potential researches.

II. System Model

In this section, we present a framework of C-RAN based licensed and unlicensed interoperable network, which consists of three main components, namely, remote radio head (RRH) network, fronthaul network, and baseband unit (BBU) pool, as shown in Fig. 1. The RRH network is deployed with both macro-BSs and dense micro-BSs to provide the licensed and unlicensed spectra coverage, respectively. By consolidating and migrating the functions of BSs, including baseband processing, storage, computation and management, to BBU pool, while only leaving RF units in the front-end, the complexity of RRH network could be greatly reduced [9]. Moreover, energy consumption, as well as network deployment and operational costs could be significantly decreased [25]. With cloud technologies, BBU pool can implement these BS functions efficiently. More importantly, centralized resource management for all macro-BSs and micro-BSs in the RRH network can be realized, which could bring in higher spectrum utilization, and better quality of service (QoS) or QoE. Due to these benefits, employing C-RAN is necessary to make our designed networks and proposed schemes effective for practical use. Fronthaul network is in charge of establishing the connection between RRH network and BBU pool, which can be realized over heterogeneous physical medium, including wireless point-to-point transmission, cable, fiber, etc [8].

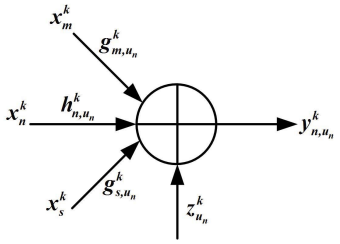

Fig. 2. Received Signal on unlicensed channel.

Because of low transmission reliability of unlicensed spectra, control information with high reliability requirements should be carried by reliable licensed spectra rather than unlicensed spectra. Thus, the control/data decoupled architecture, as a fundamental reliability guarantee for each user, should be employed in our proposed architecture, in which control information is supported by macro-BSs on limited licensed spectra to guarantee reliable transmissions, while micro-BSs can only transmit data information on wide bandwidth unlicensed spectra to enhance system capacity [8]. If resources are adequate, licensed spectra are also allowed to carry part of data information to improve network reliability level.

In this paper, as case study, we consider a licensed and unlicensed interoperable network with a macro-BS and dense micro-BSs, and only downlink transmissions will be studied. The main notations are shown as follows. $\mathbf{N} = \{n \,|n = 1,\ 2, \cdots, N\}$ is the set of micro-BSs or microcells. $\mathbf{\Omega}_n = \{u_n \,|u_n = 1, 2, \cdots, U_n\}$ and $\mathbf{\Omega} = \{\Omega_1, \cdots, \Omega_N\} = \{u_n \,|u_n = 1, \cdots, U\}$ denote the sets of users within microcell n and macrocell, respectively. $\mathbf{S} = \{s \,|s = 1, 2, \cdots, S\}$ stands for the set of interference sources, such as Wi-Fi, LTE-U, LAA, etc. $\Delta_{li} = \{l \,|l = 1, 2, \cdots, L\}$ and $\Delta_{unli,n} = \{k \,|k = 1, 2, \cdots, K\}$ represents the sets of licensed channels and the unlicensed channels used in microcell n, respectively.

Two kinds of interferences will be encountered on an unlicensed channel, as shown in Fig. 2. One is the interference among microcells, namely, intra-system interference. With centralized management by BBU pool, the intra-system interference is controllable. The kind of interference caused by other wireless devices, so-called inter-system interference, is uncontrollable, the strength and arrival of which are random and unpredictable in time, frequency and space [26]. The received signal of user u_n on unlicensed channel k, which has been allocated to u_n, can be calculated as

$$y_{n,u_n}^k = x_n^k h_{n,u_n}^k + \sum_{m\in\mathbf{N}, m\neq n} x_m^k g_{m,u_n}^k + \sum_{s\in\mathbf{S}} x_s^k g_{s,u_n}^k + z_{u_n}^k, \tag{1}$$

where x_n^k is the desired signals transmitted by micro-BS n on unlicensed channel k. x_m^k and x_s^k represent the intra-system and inter-system interference signals from micro-BS m and interference source s, respectively. h_{n,u_n}^k, g_{m,u_n}^k and g_{s,u_n}^k stand for the gains of the links from n to user u_n, from m to u_n and from s to u_n , respectively. z_{n,u_n}^k denotes the received additive white Gaussian noise (AWGN).

Let p_{n,u_n}^k, p_{m,u_m}^k and p_s^k represent the transmit power of n, m and s on k, respectively. u_n and u_m are the desired users which k is allocated with in microcell n and m, respectively. Accordingly, the signal to interference plus noise ratio (SINR) at u_n on k can be given by

$$r_{n,u_n}^k = \frac{p_{n,u_n}^k \cdot \left|h_{n,u_n}^k\right|^2}{\underbrace{\sum_{m\in\mathbf{N}, m\neq n} p_{m,u_m}^k \left|h_{m,u_n}^k\right|^2}_{\substack{controllable\\ interference}} + \underbrace{\sum_{s\in\mathbf{S}} p_s^k \left|h_{s,u_n}^k\right|^2}_{\substack{uncontrollable\\ interference}} + \underbrace{B\cdot N_0}_{noise}}, \tag{2}$$

where N_0 and B stand for noise spectral density and channel bandwidth, respectively.

Due to spectrum regulation, it can be assumed that licensed spectra would not suffer from any interference from other wireless devices. Besides, to simplify calculation, we assume that the interference from adjacent macro-BSs can be ignored by reasonable network planning. Therefore, the received signal and SINR on licensed channel l for u_n can be expressed as

$$y_{u_n}^l = x^l h_{u_n}^l + z^l, \tag{3}$$

$$r_{u_n}^l = \frac{p_{u_n}^l \left|h_{u_n}^l\right|^2}{B\cdot N_0}, \tag{4}$$

where x^l and $p_{u_n}^l$ denote desired signals and power transmitted by macro-BS on l, respectively. $h_{u_n}^l$ is the channel gain of the link from macro-BS to u_n.

III. Interference Power Estimation Method, and Utility Definitions of Cost and Reliability

In this section, an interference power estimation method is proposed to more accurately estimate channel states. To facilitate the cost-reliability tradeoff study, cost and reliability utilities for licensed and unlicensed channels will be defined.

A. Interference Power Estimation Method

Uncontrollable interference on unlicensed spectra is always coming from two sorts of interference sources. One is from opportunistic access systems, such as Wi-Fi devices with carrier sense multiple access with collision avoidance (CSMA/CA) [27], and cognitive radio (CR) devices [28]. The other is from spectrum sharing systems, such as LAA and LTE-U devices. Thus, uncontrollable interference power may be hybrid signals from different systems with different spectrum access mechanisms, which make it very complex and its variation rules hard to grasp. For this reason, Grey Markov chain prediction model will be used to estimate it, which integrates the advantages of both Grey theory and Markov chain prediction model, and can precisely predict such a dynamic systems with both tendency and randomness, respectively [29], [30]. In this paper, the predicted object is the overall interference power mixed with uncontrollable interference and noise, which cannot be distinguished by spectrum sensing. Measured interference power can be obtained by sensing blank slots or time-frequency resource blocks embedded in

unlicensed channels [31]. Let $I_{u_n}^k(t) = \sum_{s\in\mathbf{S}} p_s^k(t)\left|h_{s,u_n}^k(t)\right|^2 + B\cdot N_0$ be measured interference power on unlicensed channel k sensed by user u_n at time t. Assume that feedback delay is τ, which means that resource allocation for wireless transmission at $t+\tau$ is performed based on channel state measurement at t. The gap between the measured interference power $I_{u_n}^k(t)$ and actual one $I_{u_n}^k(t+\tau)$ may significantly degrade resource allocation effectiveness and transmission performance at $t+\tau$. To accurately estimate channel states, we input current and historic measured interference power into the Grey Markov chain prediction model to obtain predicted one for time $t+\tau$, $\tilde{I}_{u_n}^k(t+\tau)$, which is described as follows.

Step one: Input current and historic measured interference power into GM (1,1) model, and output initial predicted values of $H+2$ moments from time $t-H\tau$ to $t+\tau$, $\hat{I}_{u_n}^k(t')$, $t' = t-H\tau,\cdots,t,t+\tau$. Then, calculate residual error between the initial predicted and actual values of $H+1$ moments from $t-H\tau$ to t by $e_{u_n}^k(t') = I_{u_n}^k(t') - \hat{I}_{u_n}^k(t')$, $t' = t-H\tau,\cdots,t$.

Step two: By dividing state, calculating state transition probability, and determining the most likely state, we can obtain the most likely residual error of predicted time $t+\tau$, $\tilde{e}_{u_n}^k(t+\tau)$, the detailed derivation process of which sees Appendix A. With $\tilde{e}_{u_n}^k(t+\tau)$, the predicted interference power can be derived as

$$\tilde{I}_{u_n}^k(t+\tau) = \hat{I}_{u_n}^k(t+\tau) + \tilde{e}_{u_n}^k(t+\tau). \tag{5}$$

B. Cost Utility

Building on the definitions in [16], we define a unified cost utility for a licensed/unlicensed channel as

$$c = c_P\cdot p + c_{li}/c_{unli}. \tag{6}$$

where c_p and p denote the cost per joule (monetary unit/J) and the power (W) consumed by transmitting a channel resource. c_{li}/c_{unli} represents overall costs not related to power consumption, including hardware operational and spectrum licensing costs, of a licensed/unlicensed channel. Because of costly spectrum license, c_{li} would substantially exceed c_{unli}.

C. Reliability Utility

The ideal reliability utility should reflect actual channel states [32], [33]. However, in practical operation, when resource allocation needs to be made, the actual channel state is always unknown and can only depend on the measured one. This makes resource allocation inaccurate and less effective, especially in a wireless environment with uncontrollable interference. To more accurately reflect potential transmission reliability of channels, apart from current channel measurement, the risk for inaccuracy of measured channel states should be also considered in channel reliability utilities. Thus, based on the original definitions in [34], we define a reliability utility, in which a channel reliability estimation based on measured channel states, and an average difference degree between measured and actual channel states, also referred to as channel instability statistic, are taken as reward and pricing functions, respectively. According to [35], proper utility functions should exhibit three main properties, including twice differentiability, monotonicity and concavity/convexity. Accordingly, for user u_n on unlicensed channel k, the reward function is defined by $10\cdot\log_{10}(1+SINR_{n,u_n}^k(t))$, where $SINR_{n,u_n}^k(t) = \frac{p_{n,u_n}^k(t)\cdot\left|h_{n,u_n}^k(t)\right|^2}{\sum_{m\in\mathbf{N},m\neq n} p_{m,u_m}^k(t)\cdot\left|h_{m,u_n}^k(t)\right|^2 + I_{u_n}^k(t)}$ stands for achievable received signal SINR under p_{n,u_n}^k. We employ $\log_2(1+\frac{\left|I_{u_n}^k(t')-I_{u_n}^k(t'-\tau)\right|}{\Delta I_{ref}})$ as a criterion of channel instability to characterize the difference degree between measured and actual channel states, where ΔI_{ref} is a referenced gap. Apparently, the instability criterion experiences logarithmic increase with the growth of the gap $\left|I_{u_n}^k(t') - I_{u_n}^k(t'-\tau)\right|$. As a long-term statistic, we define the pricing function as the weighted mean of the channel instability criteria at previous $J+1$ moments, which can be calculated as

$$DoI_{u_n}^k(t) = \frac{\sum_{t'=t-J\tau}^{t}(1-a^{J+1-\frac{t-t'}{\tau}})\cdot\log_2(1+\frac{\left|I_{u_n}^k(t')-I_{u_n}^k(t'-\tau)\right|}{\Delta I_{ref}})}{\sum_{t'=t-J\tau}^{t}(1-a^{J+1-\frac{t-t'}{\tau}})}, \tag{7}$$

where $a=0.7$ in this paper, and the pricing function is more sensitive to the instability criteria of the moments closer to t with higher weights.

Here, the reliability utility is defined as

$$\begin{aligned} &UoR_{n,u_n}^k(t)\\ &= 10\cdot\log_{10}(1+SINR_{n,u_n}^k(t)) - DoI_{u_n}^k(t)\\ &= 10\cdot\log_{10}(1+\frac{p_{n,u_n}^k(t)\cdot\left|h_{n,u_n}^k(t)\right|^2}{\sum_{m\in\mathbf{N},m\neq n} p_{m,u_m}^k(t)\cdot\left|h_{m,u_n}^k(t)\right|^2 + I_{u_n}^k(t)})\\ &\quad - \kappa\cdot\frac{\sum_{t'=t-J\tau}^{t}(1-a^{J+1-\frac{t-t'}{\tau}})\cdot\log_2(1+\frac{\left|I_{u_n}^k(t')-I_{u_n}^k(t'-\tau)\right|}{\Delta I_{ref}})}{\sum_{t'=t-J\tau}^{t}(1-a^{J+1-\frac{t-t'}{\tau}})}, \end{aligned} \tag{8}$$

where κ is a weight to adjust pricing factor. With our proposed predicted interference power, the corresponding reliability utility can be expressed by

$$\begin{aligned} &UoR_{n,u_n}^k(t)\\ &= 10\cdot\log_{10}(1+\frac{p_{n,u_n}^k(t)\cdot\left|h_{n,u_n}^k(t)\right|^2}{\sum_{m\in\mathbf{N},m\neq n} p_{m,u_m}^k(t)\cdot\left|h_{m,u_n}^k(t)\right|^2 + \tilde{I}_{u_n}^k(t+\tau)})\\ &\quad - \kappa\cdot\frac{\sum_{t'=t-J\tau}^{t}(1-a^{J+1-\frac{t-t'}{\tau}})\cdot\log_2(1+\frac{\left|I_{u_n}^k(t')-\tilde{I}_{u_n}^k(t')\right|}{\Delta I_{ref}})}{\sum_{t'=t-J\tau}^{t}(1-a^{J+1-\frac{t-t'}{\tau}})}. \end{aligned} \tag{9}$$

Under the assumption of no interference suffered, low mobility and flat fading channel, we can suppose that the

measured channel states are approximately equal to the actual one on licensed channels, and the channel instability value is zero. Thus, for user u_n on licensed channel l, the reliability utility can be given by

$$UoR^{l}_{n,u_n} = 10 \cdot \log_{10}(1 + \frac{p^{l}_{u_n} \cdot |h^{l}_{u_n}|^2}{B \cdot N_0}). \quad (10)$$

IV. Cost Versus Reliability

Assume that Φ_{u_n} and Ψ_{u_n} represent the set of the unlicensed and licensed channels allocated to u_n, respectively. In order to ensure each user allocated with adequate wireless resources to meet its data rate requirements, we have an achievable data rate constraint for each user as below.

$$\sum_{k\in\Phi_{u_n}} B\log_2(1+\tilde{r}^{k}_{n,u_n}) + \sum_{l\in\Psi_{u_n}} B\log_2(1+r^{l}_{u_n}) \geq R^{req,tot}_{u_n}, \quad \forall u_n \in \Omega \quad (11)$$

where $R^{req,tot}_{u_n}$ represents the total data rate requirements, including both control and data information, for u_n. $\tilde{r}^{k}_{n,u_n} = \frac{p^{k}_{n,u_n}\cdot|h^{k}_{n,u_n}|^2}{\sum_{m\in\mathbf{N},m\neq n} p^{k}_{m,u_m}\cdot|h^{k}_{m,u_n}|^2+\tilde{I}^{k}_{u_n}}$ is the received signal SINR for u_n on k under the predicted interference power $\tilde{I}^{k}_{u_n}$. To simplify calculation, all channels used in RRH network are assumed to have the same B.

With the control/data decoupled architecture, adequate licensed resources should be allocated to each user to support control information transmission. Thus, we have

$$\sum_{l\in\Psi_{u_n}} B\cdot\log_2(1+r^{l}_{u_n}) \geq R^{req,con}_{u_n}, \forall u_n \in \Omega \quad (12)$$

where $R^{req,con}_{u_n}$ denotes the rate requirements of control information for u_n.

For energy saving, the transmit power of a macro-BS and all micro-BSs within a macrocell cannot exceed predetermined thresholds $P^{\max}_{li}$ and $P^{\max}_{unli}$, respectively. Moreover, each micro-BS should obey power limitation Γ on unlicensed spectra ruled by government. All the energy constraints can be expressed as

$$\sum_{u_n\in\Omega}\sum_{k\in\Phi_{u_n}} p^{k}_{n,u_n} \leq P^{\max}_{unli}, \quad (13a)$$

$$\sum_{u_n\in\Omega}\sum_{l\in\Psi_n} p^{l}_{u_n} \leq P^{\max}_{li}, \quad (13b)$$

$$\sum_{u_n\in\Omega_n}\sum_{k\in\Phi_{u_n}} p^{k}_{n,u_n} \leq \Gamma. \quad \forall n \in \mathbf{N} \quad (13c)$$

A. Cost-Reliability Tradeoff by Minimizing Cost for a Given Reliability Constraint

A fundamental network-level cost-reliability tradeoff can be investigated by seeking for optimal joint licensed/unlicensed resource allocation strategy, which could minimize the cost for a given reliability. This leads to the following optimization problem with the aforementioned constraints.

$$\min \sum_{u_n\in\Omega}\left[\sum_{k\in\Phi_{u_n}}(c_P\cdot p^{k}_{n,u_n}+c_{unli}) + \sum_{l\in\Psi_{u_n}}(c_P\cdot p^{l}_{u_n}+c_{li})\right]$$

subject to

$$\sum_{u_n\in\Omega}\left[\sum_{k\in\Phi_{u_n}}\left(10\cdot\log_{10}(1+\frac{p^{k}_{n,u_n}\cdot|h^{k}_{n,u_n}|^2}{\sum_{m\in\mathbf{N},m\neq n} p^{k}_{m,u_m}\cdot|h^{k}_{m,u_n}|^2+\tilde{I}^{k}_{u_n}}) - \kappa\cdot DoI^{k}_{u_n}\right) + \sum_{l\in\Psi_{u_n}} 10\cdot\log_{10}(1+\frac{p^{l}\cdot|h^{l}_{u_n}|^2}{B\cdot N_0})\right] = Rel,$$

$$(11),\ (12),\ (13a)-(13c). \quad (14)$$

The optimization problem in (14) involves both power distribution with continuous variables and channel assignment with binary variables, also referred to as mixed binary integer programming problem, which is generally hard to obtain the optimal solution [10]. In this paper, we adopt the Per-Stage Dual-Variable Update (PSDU) scheme, originally introduced in [36], to solve such an optimization problem. Through Lagrange relaxation, the Lagrangian with respect to transmit power $\mathbf{P}_{unli} := \{p^{k}_{n,u_n}\}_{u_n\in\Omega,k\in\Phi_{u_n}}$ and $\mathbf{P}_{li} := \{p^{l}_{u_n}\}_{u_n\in\Omega,l\in\Psi_{u_n}}$ is shown in (15) at the bottom of the next page, where $\boldsymbol{\mu} := \{\mu_{u_n}\}_{u_n\in\Omega}$, $\boldsymbol{\alpha} := \{\alpha_{u_n}\}_{u_n\in\Omega}$, θ, $\boldsymbol{\eta} := \{\eta_n\}_{n\in\mathbf{N}}$, λ and γ are the Lagrange multipliers for the constraints. Accordingly, the dual problem can be given by

$$\max\ D_1(\boldsymbol{\mu},\boldsymbol{\alpha},\theta,\boldsymbol{\eta},\lambda,\gamma)$$
$$\text{subject to } \boldsymbol{\mu}\geq 0,\ \boldsymbol{\alpha}\geq 0,\ \theta\geq 0,\ \boldsymbol{\eta}\geq 0,\ \lambda\geq 0 \text{ and } \gamma\geq 0, \quad (16)$$

where $D_1(\boldsymbol{\mu},\boldsymbol{\alpha},\theta,\boldsymbol{\eta},\lambda,\gamma) = \inf_{\mathbf{P}_{unli},\mathbf{P}_{li}} L_1(\mathbf{P}_{unli},\mathbf{P}_{li},\boldsymbol{\mu},\boldsymbol{\alpha},\theta,\boldsymbol{\eta},\lambda,\gamma)$ is the Lagrange dual function. To solve (16), the infimum of (15) needs to be obtained for given Lagrange multipliers. We use the primal-dual decomposition scheme to get optimal transmit power, which can achieve the infimum [31]. With the primal-dual decomposition scheme, the joint optimization problem will be decomposed into two convex single-variable optimization problems with only one kind of variables ($\mathbf{P}_{unli}$ or $\mathbf{P}_{li}$) involved, which can be solved by the Karush-Kuhn-Tucker (KKT) conditions.

Since the PSDU is an iterative algorithm, we employ the iterative water-filling scheme to update the transmit power at each iteration. At iteration s', the transmit power update can be derived by

$$p^{k(s')}_{n,u_n} = \left[\frac{\mu^{(s'-1)}_{u_n}\cdot\frac{B}{\ln 2}+\theta^{(s'-1)}\cdot\frac{10}{\ln 10}}{c_p+\lambda^{(s'-1)}+\eta^{(s'-1)}_n} - \frac{\sum_{m\in\mathbf{N},m\neq n} p^{k(s'-1)}_{m,u_m}\cdot|h^{k}_{m,u_n}|^2+\tilde{I}^{k}_{u_n}}{|h^{k}_{n,u_n}|^2}\right]^{+}_{0}, \quad (17)$$

$$p^{l(s')}_{u_n} = \left[\frac{(\mu^{(s'-1)}_{u_n}+\alpha^{(s'-1)}_{u_n})\cdot\frac{B}{\ln 2}+\theta^{(s'-1)}\cdot\frac{10}{\ln 10}}{c_p+\gamma^{(s'-1)}} - \frac{B\cdot N_0}{|h^{l}_{u_n}|^2}\right]^{+}_{0}, \quad (18)$$

where $[a]_0^+ = a$ if $a > 0$, otherwise $[a]_0^+ = 0$. Clearly, the Lagrange multipliers from the last iteration $s'-1$ determine the water-filling level.

The channel assignment update is carried out based on the updated transmit power $\mathbf{P}_{unli}^{(s')}$ and $\mathbf{P}_{li}^{(s')}$. Since each unlicensed channel can be only allocated to one user within a microcell, unlicensed channel k is allocated to unique $u_n^* \in \mathbf{\Omega}_n$, if

$$u_n^* = \arg\min_{u_n \in \mathbf{\Omega}_n} \Bigg\{ (c_P \cdot p_{n,u_n}^{k(s')} + c_{unli}) - \mu_{u_n}^{(s'-1)} \cdot B \cdot \log_2\Big(1 + \frac{p_{n,u_n}^{k(s')} \cdot \left|h_{n,u_n}^k\right|^2}{\sum_{m \in \mathbf{N}, m \neq n} p_{m,u_m}^{k(s')} \cdot \left|h_{m,u_n}^k\right|^2 + \tilde{I}_{u_n}^k}\Big) - \theta^{(s'-1)} \cdot \Bigg(10 \cdot \log_{10}\Big(1 + \frac{p_{n,u_n}^{k(s')} \cdot \left|h_{n,u_n}^k\right|^2}{\sum_{m \in \mathbf{N}, m \neq n} p_{m,u_m}^{k(s')} \cdot \left|h_{m,u_n}^k\right|^2 + \tilde{I}_{u_n}^k}\Big) - \kappa \cdot DoI_{u_n}^k\Bigg) + \lambda^{(s'-1)} \cdot p_{n,u_n}^{k(s')} + \eta_n^{(s'-1)} \cdot p_{n,u_n}^{k(s')} \Bigg\}. \tag{19}$$

Similarly, licensed channel l is allocated to unique $u_n^* \in \mathbf{\Omega}$ within a macrocell, if

$$u_n^* = \arg\min_{u_n \in \mathbf{\Omega}} \Bigg\{ (c_P \cdot p_{u_n}^{l(s')} + c_{li}) - (\mu_{u_n}^{(s'-1)} + \alpha_{u_n}^{(s'-1)}) \cdot B \cdot \log_2\Big(1 + \frac{p_{u_n}^{l(s')} \cdot \left|h_{u_n}^l\right|^2}{B \cdot N_0}\Big) - \theta^{(s'-1)} \cdot 10 \cdot \log_{10}\Big(1 + \frac{p_{u_n}^{l(s')} \cdot \left|h_{u_n}^l\right|^2}{B \cdot N_0}\Big) + \gamma^{(s'-1)} \cdot p_{u_n}^{l(s')} \Bigg\}. \tag{20}$$

According to (19) and (20), update Φ_{u_n} and Ψ_{u_n} for $\forall u_n \in \mathbf{\Omega}$. To maximize the Lagrange dual function (16), optimal Lagrange multipliers need to be found under the updated power distribution and channel assignment. The subgradient method [37], as a simple and effective way, is used here to update the Lagrange multipliers at iteration s', as shown in (21a)-(21f) at the top of the next page, where ε is a small step size. In summary, algorithm 1 gives an overall iteration procedure to solve the optimization problem (14).

Algorithm 1 Optimal Joint Licensed/Unlicensed Resource Allocation for Optimization Problem (14)

1. Initialization: Set $s' = 0$. Initialize Lagrange multipliers as some large enough values. Initialize $\mathbf{P}_{unli}^{(0)}$ and $\mathbf{P}_{li}^{(0)}$ by equal power distribution, namely, $p_{n,u_n}^{k(0)} = \frac{P_{unli}^{\max}}{N \cdot K}$ and $p_{u_n}^{l(0)} = \frac{P_{li}^{\max}}{L}$. Set $\Phi_{u_n} = \varnothing$ and $\Psi_{u_n} = \varnothing$ for $\forall u_n \in \mathbf{\Omega}$.

2. Iteration s'**:**

1) calculate the transmit power for $\forall u_n \in \mathbf{\Omega}$ on $\forall k \in \Delta_{unli,n}$ and $\forall l \in \Delta_{li}$, namely $p_{n,u_n}^{k(s')}$ and $p_{u_n}^{l(s')}$, according to (17) and (18), respectively.

2) For $\forall k \in \Delta_{unli,n}, n = 1 \cdots N$, allocate unlicensed channel k to u_n^* according to (19). If $p_{n,u_n^*}^{k(s')} \neq 0$, update $\Phi_{u_n^*}$ by $\Phi_{u_n^*} = \Phi_{u_n^*} \cup \{k\}$, otherwise do not assign k in this round.

3) For $\forall l \in \Delta_{li}$, allocate licensed channel l to u_n^* according to (20). If $p_{u_n^*}^{l(s')} \neq 0$, update $\Psi_{u_n^*}$ by $\Psi_{u_n^*} = \Psi_{u_n^*} \cup \{l\}$, otherwise do not assign l in this round.

4) Update Lagrange multipliers $\boldsymbol{\mu}^{(s')}$, $\boldsymbol{\alpha}^{(s')}$, $\theta^{(s')}$, $\boldsymbol{\eta}^{(s')}$, $\lambda^{(s')}$ and $\gamma^{(s')}$ by the subgradient method according to (21a)-(21f), respectively.

3. Decision: If all Lagrange multipliers converge, output the channel assignment (Φ_{u_n} and Ψ_{u_n} of $\forall u_n \in \mathbf{\Omega}$) and power distribution ($\mathbf{P}_{unli}$ and $\mathbf{P}_{li}$). Otherwise, set $s' = s'+1$, $\Phi_{u_n} = \varnothing$ and $\Psi_{u_n} = \varnothing$, and return to **2**.

V. QoE Efficiency

Enlightened by using ECE to study the SE-EE tradeoff [17], [18], we propose a QoE efficiency which is a complementary performance measure to cost and reliability. Both lowering cost and heightening reliability can improve QoE, however, enhancement of one of them always makes the deterioration of the other. Thus, maximizing

$$\begin{aligned} &L_1\left(\mathbf{P}_{unli}, \mathbf{P}_{li}, \boldsymbol{\mu}, \boldsymbol{\alpha}, \theta, \boldsymbol{\eta}, \lambda, \gamma\right) \\ &= \sum_{u_n \in \mathbf{\Omega}} \Bigg[\sum_{k \in \Phi_{u_n}} (c_P \cdot p_{n,u_n}^k + c_{unli}) + \sum_{l \in \Psi_{u_n}} (c_P \cdot p_{u_n}^l + c_{li}) \Bigg] \\ &\quad + \sum_{u_n \in \mathbf{\Omega}} \mu_{u_n} \cdot \Bigg[R_{u_n}^{req,tot} - \sum_{k \in \Phi_{u_n}} B \cdot \log_2\Big(1 + \frac{p_{n,u_n}^k \cdot \left|h_{n,u_n}^k\right|^2}{\sum_{m \in \mathbf{N}, m \neq n} p_{m,u_m}^k \cdot \left|h_{m,u_n}^k\right|^2 + \tilde{I}_{u_n}^k}\Big) - \sum_{l \in \Psi_{u_n}} B \cdot \log_2\Big(1 + \frac{p_{u_n}^l \cdot \left|h_{u_n}^l\right|^2}{B \cdot N_0}\Big) \Bigg] \\ &\quad + \sum_{u_n \in \mathbf{\Omega}} \alpha_{u_n} \cdot \Bigg[R_{u_n}^{req,con} - \sum_{l \in \Psi_{u_n}} B \cdot \log_2\Big(1 + \frac{p_{u_n}^l \cdot \left|h_{u_n}^l\right|^2}{B \cdot N_0}\Big) \Bigg] \\ &\quad + \theta \cdot \Bigg[Rel - \sum_{u_n \in \mathbf{\Omega}} \sum_{k \in \Phi_{u_n}} \Bigg(10 \cdot \log_{10}\Big(1 + \frac{p_{n,u_n}^k \cdot \left|h_{n,u_n}^k\right|^2}{\sum_{m \in \mathbf{N}, m \neq n} p_{m,u_m}^k \cdot \left|h_{m,u_n}^k\right|^2 + \tilde{I}_{u_n}^k}\Big) - \kappa \cdot DoI_{u_n}^k\Bigg) - \sum_{u_n \in \mathbf{\Omega}} \sum_{l \in \Psi_{u_n}} 10 \cdot \log_{10}\Big(1 + \frac{p_{u_n}^l \cdot \left|h_{u_n}^l\right|^2}{B \cdot N_0}\Big) \Bigg] \\ &\quad + \lambda \cdot \Bigg(\sum_{u_n \in \mathbf{\Omega}} \sum_{k \in \Phi_{u_n}} p_{n,u_n}^k - P_{unli}^{\max} \Bigg) + \sum_{n \in \mathbf{N}} \eta_n \cdot \Bigg(\sum_{u_n \in \mathbf{\Omega}_n} \sum_{k \in \Phi_{u_n}} p_{n,u_n}^k - \Gamma \Bigg) + \gamma \cdot \Bigg(\sum_{u_n \in \mathbf{\Omega}} \sum_{l \in \Psi_n} p_{u_n}^l - P_{li}^{\max} \Bigg). \end{aligned} \tag{15}$$

$$\mu_{u_n}^{(s')} = \left[\mu_{u_n}^{(s'-1)} - \varepsilon \cdot \left(\sum_{k\in\Phi_{u_n}} B\cdot\log_2(1+\frac{p_n^{k(s')}\cdot\left|h_{n,u_n}^k\right|^2}{\sum\limits_{m\in\mathbf{N},m\neq n} p_{m,u_m}^{k(s')}\cdot\left|h_{m,u_n}^k\right|^2+\tilde{I}_{u_n}^k}) + \sum_{l\in\Psi_{u_n}} B\cdot\log_2(1+\frac{p^{l(s')}\cdot\left|h_{u_n}^l\right|^2}{B\cdot N_0}) - R_{u_n}^{req,tot}\right)\right]_0^+, \tag{21a}$$

$$\alpha_{u_n}^{(s')} = \left[\alpha_{u_n}^{(s'-1)} - \varepsilon \cdot \left(\sum_{l\in\Psi_{u_n}} B\cdot\log_2(1+\frac{p_{u_n}^{l(s')}\cdot\left|h_{u_n}^l\right|^2}{B\cdot N_0}) - R_{u_n}^{req,con}\right)\right]_0^+, \tag{21b}$$

$$\theta^{(s')} = \left[\theta^{(s'-1)} - \varepsilon \cdot \left(\sum_{u_n\in\Omega}\sum_{k\in\Phi_{u_n}} \left(10\cdot\log_{10}(1+\frac{p_{n,u_n}^{k(s')}\cdot\left|h_{n,u_n}^k\right|^2}{\sum\limits_{m\in\mathbf{N},m\neq n} p_{m,u_m}^{k(s')}\cdot\left|h_{m,u_n}^k\right|^2+\tilde{I}_{u_n}^k}) - \kappa\cdot DoI_{u_n}^k\right) + \sum_{u_n\in\Omega}\sum_{l\in\Psi_{u_n}} 10\cdot\log_{10}(1+\frac{p_{u_n}^{l(s')}\cdot\left|h_{u_n}^l\right|^2}{B\cdot N_0}) - Rel\right)\right]_0^+, \tag{21c}$$

$$\eta_n^{(s')} = \left[\eta_n^{(s'-1)} - \varepsilon\cdot(\Gamma - \sum_{u_n\in\Omega_n}\sum_{k\in\Phi_{u_n}} p_{n,u_n}^{k(s')})\right]_0^+, \tag{21d}$$

$$\lambda^{(s')} = \left[\lambda^{(s'-1)} - \varepsilon\cdot(P_{unli}^{\max} - \sum_{u_n\in\Omega}\sum_{k\in\Phi_{u_n}} p_{n,u_n}^{k(s')})\right]_0^+, \tag{21e}$$

$$\gamma^{(s')} = \left[\gamma^{(s'-1)} - \varepsilon\cdot(P_{li}^{\max} - \sum_{u_n\in\Omega}\sum_{l\in\Psi_n} p_{u_n}^{l(s')})\right]_0^+. \tag{21f}$$

QoE measure could be a good way to find an excellent balance between cost and reliability.

A. Definition of QoE Efficiency Utility

Generally, three main types of performance indicators impact on QoE, namely, data rate, cost and the relevant indicators related to reliability, such as delay, signal error probability, link outage probability, etc [38]. In this paper, we formulate the constraint (11) to guarantee data rate requirements of each user to be satisfied, therefore it can be assumed that the data rate for each user has the same influence on QoE. To simplify calculation, we define a QoE efficiency utility with only cost and reliability considered. Among numerous existing utility functions, we found that the sigmoidal (S-shaped) function [35] is a proper and simple function to form QoE utility functions shown as follows.

$$u_1(c) = \frac{1}{1+e^{\xi_1(c-c_0)}}, \quad \xi_1 > 0, \tag{22}$$

$$u_2(UoR) = \frac{1}{1+e^{\xi_2(UoR_0-UoR)}}, \quad \xi_2 > 0, \tag{23}$$

where c and UoR represent the values of cost and reliability utilities, respectively. ξ_1 and ξ_2 are sensitivity parameters, by tuning which the sensitivity of utility function to variables can be adjusted. c_0 and UoR_0 are reference points which are always regarded as satisfaction thresholds. The sensitivity parameters and reference points determine the steepness and center of the S-shaped function, respectively. From (22) and (23), we can see that the growth of cost and reliability has the opposite effect on QoE utility, namely, lowering and heightening it, respectively. Without loss of generality, we adopt the most common multi-criterion utility functions, namely, the additive aggregate function [35], to define the QoE efficiency utility for user u_n as

$$\begin{aligned} QoEE_{u_n} &= \phi_{u_n,0}\cdot\left[u_1\left(\sum_{k\in\Phi_{u_n}}(c_P\cdot p_{n,u_n}^k + c_{unli}) + \sum_{l\in\Psi_{u_n}}(c_P\cdot p_{u_n}^l + c_{li})\right)\right] + \phi_{u_n,1} \\ &\times\left[u_2\left(\sum_{k\in\Phi_{u_n}}\left(10\log_{10}(1+\frac{p_{n,u_n}^k\cdot\left|h_{n,u_n}^k\right|^2}{\sum\limits_{m\in\mathbf{N},m\neq n} p_{m,u_m}^k\cdot\left|h_{m,u_n}^k\right|^2+\tilde{I}_{u_n}^k}) - \kappa\cdot DoI_{u_n}^k\right) + \sum_{l\in\Psi_{u_n}} 10\log_{10}(1+\frac{p_{u_n}^l\left|h_{u_n}^l\right|^2}{B\cdot N_0})\right)\right], \end{aligned} \tag{24}$$

where $\phi_{u_n,0} \geq 0$ and $\phi_{u_n,1} \geq 0$ denote preference weights of cost and reliability, respectively, with $\phi_{u_n,0} + \phi_{u_n,1} = 1$. The first term and the second term in (24) represent QoE gain obtained from cost and reliability, respectively.

B. Cost-Reliability Tradeoff by Maximizing QoE Efficiency

To investigate the network-level cost-reliability tradeoff, optimization objective is to maximize the global QoE efficiency, namely, the summation of the QoE efficiency utilities of all users $u_n \in \Omega$. Moreover, the equations of (11), (12) and (13a)-(13c) will be employed as the constraints. Accordingly, the optimization problem can be

formulated as follows.

$$\max \sum_{u_n\in\Omega}\Bigg\{\phi_{u_n,0}\cdot u_1\Bigg(\sum_{k\in\Phi_{u_n}}(c_P\cdot p^k_{n,u_n}+c_{unli}) + \sum_{l\in\Psi_{u_n}}(c_P\cdot p^l_{u_n}+c_{li})\Bigg)+\phi_{u_n,1}\cdot u_2\Bigg(\sum_{k\in\Phi_{u_n}}(10\cdot\log_{10}(1 + \frac{p^k_{n,u_n}\cdot\left|h^k_{n,u_n}\right|^2}{\sum\limits_{m\in\mathbf{N},m\neq n}p^k_{m,u_m}\cdot\left|h^k_{m,u_n}\right|^2+\tilde{I}^k_{u_n}})-\kappa\cdot DoI^k_{u_n}) + \sum_{l\in\Psi_{u_n}}10\cdot\log_{10}(1+\frac{p^l_{u_n}\cdot\left|h^l_{u_n}\right|^2}{B\cdot N_0})\Bigg)\Bigg\}$$
$$\text{subject to (11), (12), (13}a\text{)} - \text{(13}c\text{).} \tag{25}$$

Similar to (14), we still face a mixed binary integer programming problem in (25), and PSDU is also used to solve it. The Lagrangian with respect to $\mathbf{P}_{unli}$ and $\mathbf{P}_{li}$ is given in (26) shown at the top of the next page, whose dual function is $D_2(\boldsymbol{\mu},\boldsymbol{\alpha},\boldsymbol{\eta},\lambda,\gamma)=\sup\limits_{\mathbf{P}_{unli},\mathbf{P}_{li}} L_2(\mathbf{P}_{unli},\mathbf{P}_{li},\boldsymbol{\mu},\boldsymbol{\alpha},\boldsymbol{\eta},\lambda,\gamma)$.

The traditional solutions for constrained optimization problem, e.g., KKT condition, would encounter the NP-hard problem in (26). Thus, we use fixed-point method to update the transmit power distribution at each iteration. By taking the first-order derivative of (26) and setting it to zero, we can obtain optimal $\mathbf{P}_{unli}$ and $\mathbf{P}_{li}$ for given Lagrange multipliers at iteration s' as follows.

$$p^{k(s')}_{n,u_n}=\Bigg[\frac{\mu^{(s'-1)}_{u_n}\cdot\frac{B}{\ln 2}+\phi_{u_n,1}\cdot\beta_0(p^{k(s'-1)}_{n,u_n})\cdot\frac{10}{\ln 10}}{\lambda^{(s'-1)}+\eta^{(s'-1)}_n-\phi_{u_n,0}\cdot\alpha_0(p^{k(s'-1)}_{n,u_n})\cdot c_p} - \frac{\sum\limits_{m\in\mathbf{N},m\neq n}p^{k(s'-1)}_{m,u_m}\cdot\left|h^k_{m,u_n}\right|^2+\tilde{I}^k_{u_n}}{\left|h^k_{n,u_n}\right|^2}\Bigg]^+_0, \tag{27}$$

$$p^{l(s')}_{u_n}=\Bigg[\frac{(\mu^{(s'-1)}_{u_n}+\alpha^{(s'-1)}_{u_n})\cdot\frac{B}{\ln 2}+\phi_{u_n,1}\cdot\beta_1(p^{l(s'-1)}_{u_n})\cdot\frac{10}{\ln 10}}{\gamma^{(s'-1)}-\phi_{u_n,0}\cdot\alpha_1(p^{l(s'-1)}_{u_n})\cdot c_p} - \frac{B\cdot N_0}{\left|h^l_{u_n}\right|^2}\Bigg]^+_0, \tag{28}$$

where $\alpha_0(p^l_{u_n})$, $\beta_0(p^k_{n,u_n})$, $\alpha_1(p^l_{u_n})$ and $\beta_1(p^k_{n,u_n})$ are presented as (29a)-(29d) shown at the top of the next page.

With the updated power distribution, channel assignment at iteration s' is performed as follows. Unlicensed channel k is allocated to $u^*_n\in\boldsymbol{\Omega}_n$, if

$$u^*_n = \arg\max_{u_n\in\boldsymbol{\Omega}_n}\Bigg\{\phi_{u_n,0}\cdot u_3\Bigg(c_P\cdot p^{k(s')}_{n,u_n}+c_{unli}\Bigg) +\phi_{u_n,1}\cdot u_4\Bigg(10\cdot\log_{10}(1+\frac{p^{k(s')}_{n,u_n}\left|h^k_{n,u_n}\right|^2}{\sum\limits_{m\in\mathbf{N},m\neq n}p^{k(s')}_{m,u_m}\left|h^k_{m,u_n}\right|^2+\tilde{I}^k_{u_n}}) -\kappa DoI^k_{u_n}\Bigg)+\mu^{(s'-1)}_{u_n}\log_2(1+\frac{p^{k(s')}_{n,u_n}\left|h^k_{n,u_n}\right|^2}{\sum\limits_{m\in\mathbf{N},m\neq n}p^{k(s')}_{m,u_m}\left|h^k_{m,u_n}\right|^2+\tilde{I}^k_{u_n}}) -\lambda^{(s'-1)}\cdot p^{k(s')}_{n,u_n}-\eta^{(s'-1)}_n\cdot p^{k(s')}_{n,u_n}\Bigg\}. \tag{30}$$

Algorithm 2 Optimal Joint Licensed/Unlicensed Resource Allocation for Optimization Problem (25)

1. Initialization is same with Algorithm 1.

2. Iteration s':

1) Update the transmit power for $\forall u_n\in\Omega$ on $\forall k\in\Delta_{unli,n}$ and $\forall l\in\Delta_{li}$ by fixed-point method according to (27) and (28), respectively.

2) Update the channel assignment for $\forall k\in\Delta_{unli,n}$, $n=1\cdots N$, and $\forall l\in\Delta_{li}$ according to (30) and (31), respectively. The updates of $\Phi_{u^*_n}$ and $\Psi_{u^*_n}$ are same with Algorithm 1.

3) Update the Lagrange multipliers by subgradient method according to (21a), (21b) and (21d)-(21f).

3. Decision is same with Algorithm 1.

Licensed channel l is allocated to $u^*_n\in\boldsymbol{\Omega}$, if

$$u^*_n=\arg\max_{u_n\in\boldsymbol{\Omega}}\Bigg\{\phi_{u_n,0}\cdot u_3\Bigg(c_P\cdot p^{l(s')}_{u_n}+c_{li}\Bigg) +\phi_{u_n,1}\cdot u_4\Bigg(10\log_{10}(1+\frac{p^{l(s')}_{u_n}\cdot\left|h^l_{u_n}\right|^2}{B\cdot N_0})\Bigg)+(\mu^{(s'-1)}_{u_n} +\alpha^{(s'-1)}_{u_n})\cdot B\log_2(1+\frac{p^{l(s')}_{u_n}\left|h^l_{u_n}\right|^2}{BN_0})-\gamma^{(s'-1)}\cdot p^{l(s')}_{u_n}\Bigg\}. \tag{31}$$

Since $u_1(\bullet)$ and $u_2(\bullet)$ in (22) and (23) are used to assess the QoE metric of all channels allocated to one user, the corresponding reference threshold c_0 and UoR_0 are too big to assess that of one single channel. Therefore, in (30) and (31), we adopt $u_3(\bullet)$ and $u_4(\bullet)$ to calculate the QoE metric of one single channel with smaller reference threshold c_1 and UoR_1, respectively. With the updated power and channel allocation, we can attain the supremum of Lagrangian for given Lagrange multipliers. To minimize the dual function, we update the Lagrange multipliers by the subgradient method. To sum up, an overall iteration procedure to solve (25) is described in algorithm 2.

VI. Simulation Results and Analysis

By conducting simulation study, we demonstrate the effectiveness of our proposed interference power estimation method and defined reliability utility. In addition, the simulation results of two tradeoff methods are presented to evaluate the cost-reliability tradeoff for licensed and unlicensed interoperable networks.

A. Simulation Setup

We consider a licensed and unlicensed interoperable network with a macro-BS and $N=19$ micro-BSs as shown in Fig. 3. U_n=10 users are randomly distributed in each microcell, totally $U=190$ users in macrocell. The radiuses of macrocell and microcell are 1200m and 275m, respectively. To simplify calculation, we assume that each user has equal total data rate requirement $R^{req,tot}_{u_n}=50$Mbits/s and equal control information rate requirement $R^{req,con}_{u_n}=3$Mbits/s. Other simulation parameters are listed in Table I.

$$
\begin{aligned}
&L_2\left(\mathbf{P}_{unli}, \mathbf{P}_{li}, \boldsymbol{\mu}, \boldsymbol{\alpha}, \boldsymbol{\eta}, \lambda, \gamma\right) \\
&= \sum_{u_n \in \Omega} \Bigg\{ \phi_{u_n,0} \cdot u_1 \Bigg(\sum_{k \in \Phi_{u_n}} \left(c_P \cdot p^k_{n,u_n} + c_{unli}\right) + \sum_{l \in \Psi_{u_n}} \left(c_P \cdot p^l_{u_n} + c_{li}\right) \Bigg) \\
&\quad + \phi_{u_n,1} \cdot u_2 \Bigg(\sum_{k \in \Phi_{u_n}} \left(10 \cdot \log_{10}\left(1 + \frac{p^k_{n,u_n} \cdot \left|h^k_{n,u_n}\right|^2}{\sum\limits_{m \in \mathbf{N}, m \neq n} p^k_{m,u_m} \cdot \left|h^k_{m,u_n}\right|^2 + \tilde{I}^k_{u_n}}\right) - \kappa \cdot DoI^k_{u_n}\right) + \sum_{l \in \Psi_{u_n}} 10 \cdot \log_{10}\left(1 + \frac{p^l_{u_n} \cdot \left|h^l_{u_n}\right|^2}{B \cdot N_0}\right) \Bigg) \Bigg\} \\
&\quad + \sum_{u_n \in \Omega} \mu_{u_n} \cdot \Bigg[\sum_{k \in \Phi_{u_n}} B \cdot \log_2\left(1 + \frac{p^k_{n,u_n} \cdot \left|h^k_{n,u_n}\right|^2}{\sum\limits_{m \in \mathbf{N}, m \neq n} p^k_{m,u_m} \cdot \left|h^k_{m,u_n}\right|^2 + \tilde{I}^k_{u_n}}\right) + \sum_{l \in \Psi_{u_n}} B \cdot \log_2\left(1 + \frac{p^l_{u_n} \cdot \left|h^l_{u_n}\right|^2}{B \cdot N_0}\right) - R^{req,tot}_{u_n} \Bigg] \\
&\quad + \sum_{u_n \in \Omega} \alpha_{u_n} \cdot \Bigg[\sum_{l \in \Psi_{u_n}} B \cdot \log_2\left(1 + \frac{p^l_{u_n} \cdot \left|h^l_{u_n}\right|^2}{B \cdot N_0}\right) - R^{req,con}_{u_n} \Bigg] \\
&\quad + \lambda \cdot \Bigg(P^{\max}_{unli} - \sum_{u_n \in \Omega} \sum_{k \in \Phi_{u_n}} p^k_{n,u_n} \Bigg) + \sum_{n \in \mathbf{N}} \eta_n \cdot \Bigg(\Gamma - \sum_{u_n \in \Omega_n} \sum_{k \in \Phi_{u_n}} p^k_{n,u_n} \Bigg) + \gamma \cdot \Bigg(P^{\max}_{li} - \sum_{u_n \in \Omega} \sum_{l \in \Psi_n} p^l_{u_n} \Bigg). \qquad (26)
\end{aligned}
$$

$$
\alpha_0(p^k_{n,u_n}) = \frac{d\, u_1 \Bigg(c_P \cdot p^k_{n,u_n} + c_{unli} + \sum\limits_{k' \neq k, k' \in \Phi_{u_n}} \left(c_P \cdot p^{k'(s'-1)}_{n,u_n} + c_{unli}\right) + \sum\limits_{l \in \Psi_{u_n}} \left(c_P \cdot p^{l(s'-1)}_{u_n} + c_{li}\right) \Bigg)}{d\, p^k_{n,u_n}}, \qquad (29a)
$$

$$
\begin{aligned}
\beta_0(p^k_{n,u_n}) = d\, u_2 \Bigg(& 10 \cdot \log_{10}\left(1 + \frac{p^k_{n,u_n} \cdot \left|h^k_{n,u_n}\right|^2}{\sum\limits_{m \in \mathbf{N}, m \neq n} p^{k(s'-1)}_{m,u_m} \cdot \left|h^k_{m,u_n}\right|^2 + \tilde{I}^k_{u_n}}\right) - \kappa \cdot DoI^k_{u_n} \\
& + \sum_{k' \neq k, k' \in \Phi_{u_n}} \left(10 \cdot \log_{10}\left(1 + \frac{p^{k'(s'-1)}_{n,u_n} \cdot \left|h^{k'}_{n,u_n}\right|^2}{\sum\limits_{m \in \mathbf{N}, m \neq n} p^{k'(s'-1)}_{m,u_m} \cdot \left|h^{k'}_{m,u_n}\right|^2 + \tilde{I}^{k'}_{u_n}}\right) - \kappa \cdot DoI^{k'}_{u_n}\right) \\
& + \sum_{l \in \Psi_{u_n}} 10 \cdot \log_{10}\left(1 + \frac{p^{l(s'-1)}_{u_n} \cdot \left|h^l_{u_n}\right|^2}{B \cdot N_0}\right) \Bigg) / d\, p^k_{n,u_n}, \qquad (29b)
\end{aligned}
$$

$$
\alpha_1(p^l_{u_n}) = \frac{d\, u_1 \Bigg(\sum\limits_{k \in \Phi_{u_n}} \left(c_P \cdot p^{k(s'-1)}_{n,u_n} + c_{unli}\right) + c_P \cdot p^l_{u_n} + c_{li} + \sum\limits_{l' \neq l, l' \in \Psi_{u_n}} \left(c_P \cdot p^{l'(s'-1)}_{u_n} + c_{li}\right) \Bigg)}{d\, p^l_{u_n}}, \qquad (29c)
$$

$$
\begin{aligned}
\beta_1(p^l_{u_n}) = d\, u_2 \Bigg(& \sum_{k \in \Phi_{u_n}} \left(10 \cdot \log_{10}\left(1 + \frac{p^{k(s'-1)}_{n,u_n} \cdot \left|h^k_{n,u_n}\right|^2}{\sum\limits_{m \in \mathbf{N}, m \neq n} p^{k(s'-1)}_{m,u_m} \cdot \left|h^k_{m,u_n}\right|^2 + \tilde{I}^k_{u_n}}\right) - \kappa \cdot DoI^k_{u_n}\right) + 10 \cdot \log_{10}\left(1 + \frac{p^l_{u_n} \cdot \left|h^l_{u_n}\right|^2}{B \cdot N_0}\right) \\
& + \sum_{l' \neq l, l' \in \Psi_{u_n}} 10 \cdot \log_{10}\left(1 + \frac{p^{l'(s'-1)}_{u_n} \cdot \left|h^{l'(s'-1)}_{u_n}\right|^2}{B \cdot N_0}\right) \Bigg) / d\, p^l_{u_n}. \qquad (29d)
\end{aligned}
$$

For simulation, proper interference model is essential, which can be formulated as

$$
I(t+\tau) = \left[B \cdot N_0,\ I(t) + \delta(t+\tau)\right]^+_0, \qquad (32)
$$

where $\delta(t+\tau) = normrnd(0, \sigma^2) + \sum\limits_{w=1}^{\infty} w \bar{I} \frac{(\lambda_{Wi}\tau)^w}{w!} e^{-\lambda_{Wi}\tau}$ denotes unknown interference variations during the time from t to $t+\tau$. The first term stands for random interference variations caused by other cellular systems, such as LTE-U, and $normrnd(0, \sigma^2)$ obeys Gaussian distribution with mean 0 and variance σ^2. The second term is interference variations caused by Wi-Fi devices, in which interference arrival obeys Poisson distribution with arrival rate λ_{Wi}. w and $\bar{I}$ are the number of arrival Wi-Fi interference and average received interference power, respectively. Accordingly, the (32) can be rewritten as $I(t+\tau) = [B \cdot N_0,\ mormrnd(I(t) + \sum\limits_{w=1}^{\infty} w \bar{I} \frac{(\lambda_{Wi}\tau)^w}{w!} e^{-\lambda_{Wi}\tau}, \sigma^2)]^+_0$. Since $I(t)$ can be obtained by measurement, we assume that $\zeta = I(t) + \sum\limits_{w=1}^{\infty} w \bar{I} \frac{(\lambda_{wi}\tau)^w}{w!} e^{-\lambda_{wi}\tau}$ is known at any time to simplify calculation. Obviously, in the interference model, ζ and σ^2 reflect average interference

TABLE I

SIMULATION PARAMETERS [17], [39], [40]

Parameters	Values	Parameters	Values
Maximum Power Constraint for a Macro-BS $P_{unli}^{\max}$	800W(46dBm/10MHz)	Macrocell Log-normal Shadowing Fading Deviation	6dB
Maximum Power Constraint for All Micro-BSs within a Macrocell $P_{unli}^{\max}$	950W(30dBm/10MHz)	Microcell log-normal Shadowing Fading Deviation	3dB
Maximum Power Constraint for Each Micro-BS Γ	100W(33dBm/10MHz)	Referenced Gap ΔI_{ref}	1×10^{-9} mw
Channel Bandwidth B	180kHz	Thermal Noise Density N_0	-174dBm/Hz
Licensed Spectrum Bandwidth	200MHz	Power Consumption Cost c_P	4×10^{-6} monetary unit/J
Unlicensed Spectrum Bandwidth	500MHz	Operation and Spectrum Licensing Costs for a Licensed Channel c_{li}	4×10^{-4} monetary unit/J
Licensed Center Frequency	2GHz	Operation and Spectrum Licensing Costs for an Unlicensed Channel c_{unli}	4×10^{-5} monetary unit/J
Unlicensed Center Frequency	6GHz	The Element Number of Residual Error Set $H+1$	20
Macrocell Path-loss Model in Urban Scenario	$39 + 26 \cdot \log_{10}(d[m])$ $+20 \cdot \log_{10}(f_c[GHz]/5)$	The Number of Divided State D	8
Microcell Path-loss Model in Urban Scenario	$41 + 22.7 \cdot \log_{10}(d[m])$ $+20 \cdot \log_{10}(f_c[GHz]/5)$	Maximal Step in Transition Probability Table t_1+1	6
Pricing function weight κ	2	The Previous Moment Number in Channel Instability Calculation $J+1$	10

TABLE II

INTERFERENCE ENVIRONMENT DISTRIBUTION

	Region 1 with the microcells of 1,2,7,8,18 and 19	Region 2 with the microcells of 3,4,9,10,11,12 and 13	Region 3 with the microcells of 5,6,14,15,16 and 17
Frequency Band 1 5894MHz-6144MHz	$\zeta = 1 \times 10^{-8}$, $\sigma = 8 \times 10^{-9}$	$\zeta = 5 \times 10^{-9}$, $\sigma = 2 \times 10^{-9}$	$\zeta = 1 \times 10^{-8}$, $\sigma = 8 \times 10^{-9}$
Frequency Band 2 6144MHz-6394MHz	$\zeta = 5 \times 10^{-9}$, $\sigma = 2 \times 10^{-9}$	$\zeta = 1 \times 10^{-8}$, $\sigma = 8 \times 10^{-9}$	$\zeta = 5 \times 10^{-9}$, $\sigma = 2 \times 10^{-9}$

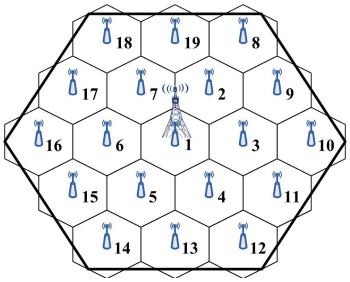

Fig. 3. Simulation model.

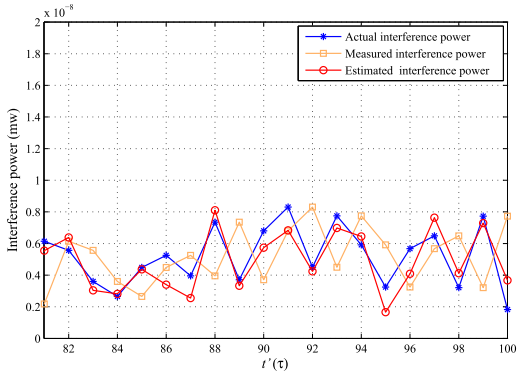

Fig. 4. Interference power versus time under $\zeta = 5\times10^{-9}$ and $\sigma = 2\times10^{-9}$.

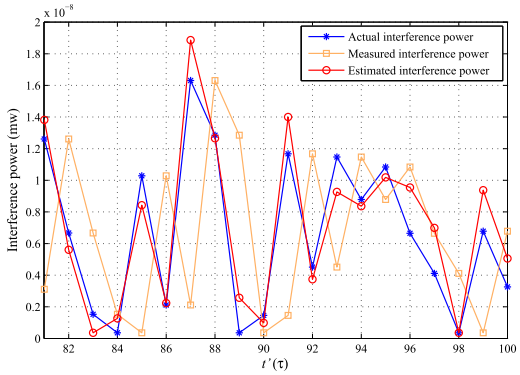

Fig. 5. Interference power versus time under $\zeta = 5\times10^{-9}$ and $\sigma = 8\times10^{-9}$.

power and the instability of unlicensed channels, respectively. To approximate practical scenario, different interference environments should be experienced in different spaces and frequencies. Thus, we divide the whole macrocell and 500MHz unlicensed spectra into three regions and two frequency bands, respectively. Besides, two sorts of interference environments are assumed, which are considered as relatively good and bad interference environments, respectively. Limited by the capability of simulation tools, we assume that all unlicensed channels on one frequency band share the same interference environments in one specific region, and the number of regions, frequency bands and interference environments are set to be relatively small. The detailed interference environment distribution used in simulation is shown in Table II.

B. Accuracy of Our Proposed Interference Power Estimation Method

In Fig. 4 and Fig. 5, we provide the predicted and measured interference power on one unlicensed channel in interference environments of $\zeta = 5 \times 10^{-9}$ and $\sigma = 2 \times 10^{-9}$, as well as $\zeta = 5\times10^{-9}$ and $\sigma = 8\times10^{-9}$, respectively. The interference power of 100 moments is simulated, in which the simulation

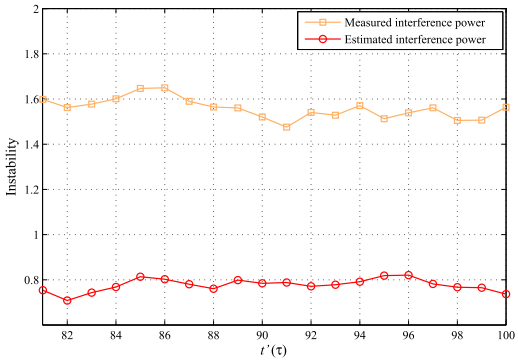

Fig. 6. Instability versus time under $\zeta = 5 \times 10^{-9}$ and $\sigma = 2 \times 10^{-9}$.

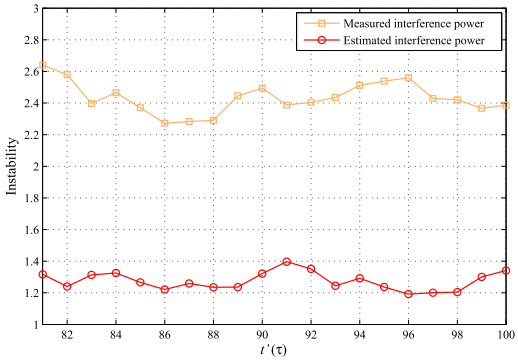

Fig. 7. Instability versus time under $\zeta = 5 \times 10^{-9}$ and $\sigma = 8 \times 10^{-9}$.

data of 20 moments from $t' = 81\tau$ to 100τ are presented. Note that actual interference power at t' is also the measured one used in resource allocation for signal transmission at $t' + \tau$. From Fig. 4 and Fig. 5, we can see that the predicted interference power (red line with circle) are more close to the actual one (blue line with star), than the measured one (yellow line with square), which indicates that our proposed interference power estimation method has better accuracy. Moreover, by comparing the Fig. 4 with Fig. 5, we find that the predicted interference power under $\sigma = 2 \times 10^{-9}$ is more close to the actual one than that under $\sigma = 8 \times 10^{-9}$. It implies that the growth of σ makes channel states become more instable and harder to estimate. This hypothesis can be testified in Fig. 6 and Fig. 7, which show the channel instability defined in (7) in the same interference environments with Fig. 4 and Fig. 5, respectively. From those, we can observe that although the growth of σ aggravates channel instability, the accurate predicted interference power can effectively ease this aggravation.

C. Impacts of Defined Reliability Utility on Resource Allocation Performance

We employ a rate-maximization optimization problem, which is the most common scheme to execute resource allocation, to testify positive impact of the defined reliability utility on resource allocation performance. To simplify calculation, only unlicensed spectra and measured channel states are considered in optimization problem, which can be

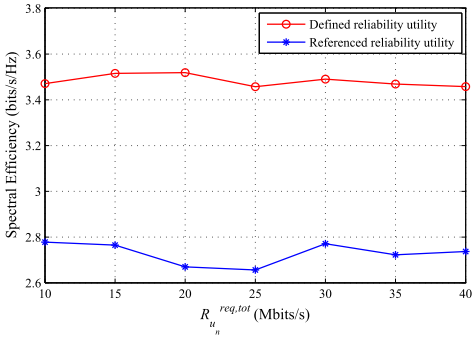

Fig. 8. Spectral efficiency versus user data rate requirements.

formulated as

$$\max \sum_{u_n \in \Omega} \sum_{k \in \Phi_{u_n}} B \log_2 \left(1 + \frac{p_{n,u_n}^k \cdot \left|h_{n,u_n}^k\right|^2}{\sum\limits_{m \in \mathbf{N}, m \neq n} p_{m,u_m}^k \cdot \left|h_{m,u_n}^k\right|^2 + I_{u_n}^k}\right)$$

subject to

$$\sum_{k \in \Phi_{u_n}} B \log_2 \left(1 + \frac{p_{n,u_n}^k \cdot \left|h_{n,u_n}^k\right|^2}{\sum\limits_{m \in \mathbf{N}, m \neq n} p_{m,u_m}^k \cdot \left|h_{m,u_n}^k\right|^2 + I_{u_n}^k}\right) \geq R_{u_n}^{req,tot}, \quad \forall u_n \in \Omega$$

$$(13a), (13c). \tag{33}$$

A low-complexity suboptimal resource allocation algorithm originally proposed in [10], is adopted to solve (33) by separating channel and power allocation, in which unlicensed channels with high reliability utilities will be prior scheduled to support user data rate transmission. The detailed solution process is described in Appendix B. To verify the effectiveness of defined reliability utility, we assume that $\zeta = 5 \times 10^{-9}$ is same for each unlicensed channel, and other parameters are same with Table II, which can make potential transmission reliability among different unlicensed channels more difficult to be distinguished. For comparison, we adopt the conventional reliability utility, which only considers measured channel states, as reference. Fig. 8 presents achievable spectral efficiency in actual interference environments for different user data rate requirements. It is easy to see that using defined reliability utility in resource allocation can bring higher spectral efficiency than referenced one. This is because with defined reliability utility, all unlicensed channels selected to transmit signals possess lower instability ($\sigma = 2 \times 10^{-9}$), while scheduled unlicensed channels with referenced one almost equally split between the channels with ($\sigma = 2 \times 10^{-9}$) and ($\sigma = 8 \times 10^{-9}$). It proves that the defined reliability utility can more accurately reflect potential transmission reliability of unlicensed spectra than the referenced one, and can effectively assist to guarantee resource allocation effectiveness.

D. Cost-Reliability Tradeoff

Fig. 9 and Fig. 10 present the convergence behaviors of Algorithm 1 and Algorithm 2, respectively. Apparently, both of them can converge with no more than 40 iterations. The choice of the Lagrange multipliers is crucial for convergence

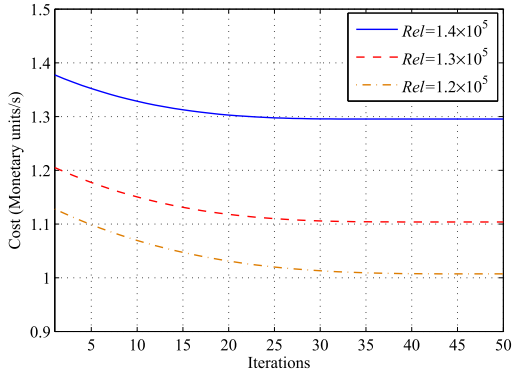

Fig. 9. Convergence behavior of Algorithm 1.

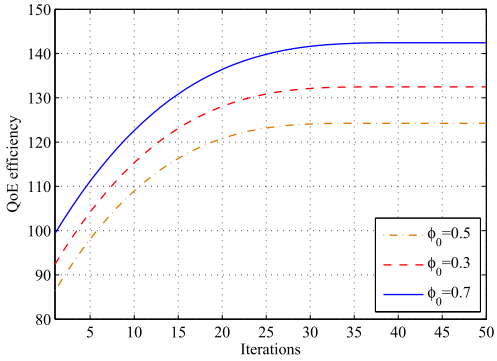

Fig. 10. Convergence behavior of Algorithm 2.

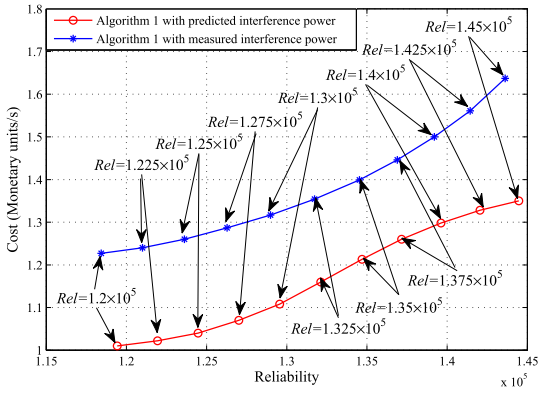

Fig. 11. Cost-reliability tradeoff by the cost minimization with a given reliability constraint.

speed. In simulation, we initialize the Lagrange multipliers with $\mu_{u_n}^{(0)} = 2 \times 10^8$, $\alpha_{u_n}^{(0)} = 1.5 \times 10^7$, $\theta^{(0)} = 7 \times 10^5$, $\eta_n^{(0)} = 5 \times 10^5$, $\lambda^{(0)} = 5 \times 10^6$ $\gamma^{(0)} = 5 \times 10^6$.

The network-level cost-reliability tradeoff is investigated using (14) as illustrated in Fig. 11. For comparison, simulation results of both the predicted and measured interference power are given. In Fig. 11, X and Y axes express, respectively, actual achieved global reliability and cost utilities obtained by employing resource allocation strategy from Algorithm 1 in actual interference environments. Since no matter the predicted or measured interference power always differs from the actual one, the actual achieved global reliability utilities are not

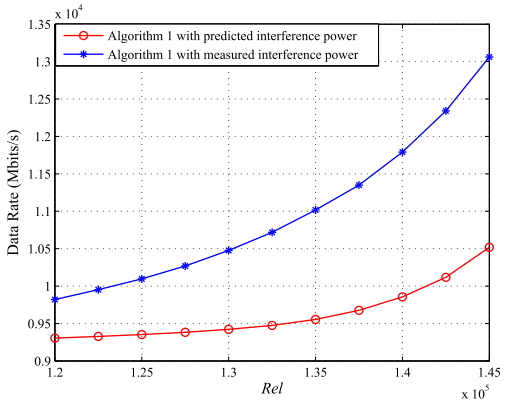

Fig. 12. The total achievable data rate versus the reliability constraint.

always equal to the given reliability constraint Rel. We can see that the cost is presented to grow with the increase of reliability, because with the growth of Rel, system haves to allocate more costly licensed channels to satisfy higher reliability requirements with higher cost caused. Moreover, using predicted interference power in Algorithm 1 can make better cost-reliability tradeoff performance, namely, the cost of that always lower than using measured one. Two reasons motivate this phenomenon. First, with predicted interference power, unlicensed channels in proposed scheme always have lower instability and higher reliability utilities. Accordingly, to achieve the same network reliability performance, more power or costly licensed channels would be invested with measured interference power utilized. Second, using predicted interference power can effectively help resource allocation guarantee effectiveness. Fig. 12 shows total achievable data rate for different $Rels$. With predicted interference power used, the achievable data rate is approximate to the total data rate requirements of 190 users, namely, 9500Mbits/s when $Rel \leq 135000$. Once $Rel > 135000$, the achievable data rate will exceed the requirements. This is because when $Rel \leq 135000$, reliability improvement is carried out by replacing unlicensed channels with licensed channels to support user data delivery. However, when $Rel > 135000$, even all licensed channels used, the reliability performance requirements still cannot be satisfied. Redundant transmission way will be aroused to provide further reliability improvement with more wireless resources allocated and extra data rate. However, when measured interference power used, the achievable data rate has already exceeded the requirements when $Rel = 120000$. Obviously, low reliability of unlicensed channels with measured interference power makes the system has to using redundant transmission way to reach the given reliability constraint at the beginning.

Fig. 13 shows the cost-reliability tradeoff by maximizing global QoE efficiency under different preference weights $\phi_{u_n,0}$ and $\phi_{u_n,1}$, $\phi_{u_n,0} + \phi_{u_n,1} = 1$ (Algorithm 2). To investigate the impact of preference weights on cost-reliability tradeoff, we assume that $\phi_{u_n,0} = \phi_0$ and $\phi_{u_n,1} = \phi_1$ for $\forall u_n \in \Omega$. Since the values of cost and reliability utilities do not lie in the same order of magnitude, the different sensitivity

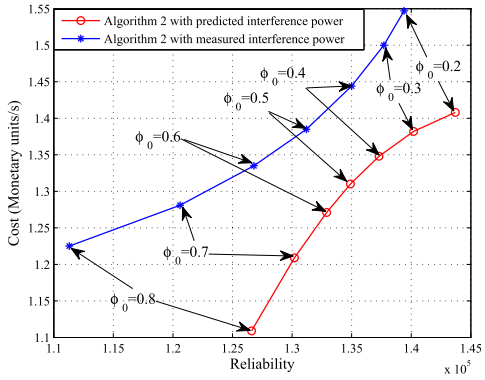

Fig. 13. Cost-reliability tradeoff by maximizing global QoE efficiency.

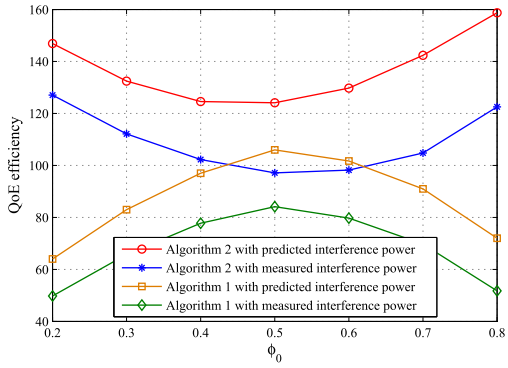

Fig. 14. The global QoE efficiency versus ϕ_0.

parameters need to be set in (22)(23), namely, $\xi_1 = 2000$ and $\xi_2 = 0.025$. Additionally, to simplify the calculation, we assume that all users share the same referenced satisfaction threshold with $c_0 = 6.8 \times 10^{-3}$, $UoR_0 = 685$, $c_1 = 6.8 \times 10^{-5}$ and $UoR_1 = 6.85$. With large ϕ_0, users prefer to economical wireless data services, which facilitates more cheap unlicensed channels allocated to provide data transmission with low cost and reliability. On the contrary, when ϕ_0 is small, system needs to schedule more costly licensed channels, and even adopt redundant transmission to meet the user preference for high reliability, resulting in high cost and reliability. By comparison, we found that using predicted interference power in Algorithm 2 always results in better cost-reliability tradeoff performance, namely lower cost than using measured one to get the same reliability. Fig. 14 presents the summation of QoE efficiency utilities of all users for different ϕ_0, and indicates that using predicted interference power lets network possess better QoE efficiency performance than using measured one. Moreover, in Fig. 14, we also testify QoE improvement performance of Algorithm 2. Since resource allocation strategy from Algorithm 1 can minimize the cost for a given reliability, which can also facilitate QoE improvement, we regard Algorithm 1 as reference. We can observe that no matter the predicted or measured interference power is used in resource allocation, the achieved global QoE efficiency of Algorithm 2 significantly exceed that of Algorithm 1, in which the reliability constraint Rel is set to be 1.3×10^5. This proves that Algorithm 2 has better QoE improvement performance.

VII. Conclusions and Future Research

In this paper, we have studied network-level cost-reliability tradeoff for a C-RAN technology and control/data decoupled architecture based 5G licensed and unlicensed interoperable network. We have proposed an interference power estimation method based on Grey Markov chain prediction model, whose simulation study indicates that it can accurately estimate channel states to assist to effective resource allocation. Then, we have investigated a fundamental cost-reliability tradeoff by minimizing cost for a given reliability. The simulation results show that with the growth of reliability constraints, system has to allocate more costly licensed channels, even using redundant transmission, to meet reliability performance requirements, causing increasingly higher cost. Moreover, the cost-reliability tradeoff is carried out by maximizing global QoE efficiency. The corresponding simulation study indicates that this tradeoff scheme can provide a good balance between cost and reliability based on the preference of users to effectively enhance network QoE performance.

It is notable that besides control information, the traffic with high reliability requirements, such as delay-sensitive and interruption-sensitive traffic, should be also carried by licensed spectra. Unfortunately, finite and scarce licensed resources are not able to support all those traffic, parts of which needed to be offloaded by unlicensed spectra with preferable reliability. Hence, the joint licensed/unlicensed resource allocation algorithm, which can guarantee the QoS of each kind of traffic, would be an interesting topic for our future researches.

Appendix A
Derivation of $\tilde{e}^k_{u_n}(t+\tau)$

Step One: The original array of a moment T' is composed of Q actual interference power $X^{(0)} = \left\{I^{k(0)}_{u_n}(T'-Q), \cdots, I^{k(0)}_{u_n}(T'-1)\right\}$. Let $X^{(1)} = \left\{I^{k(1)}_{u_n}(T'-Q), \cdots, I^{k(1)}_{u_n}(T'-1)\right\}$ be first-order accumulated generating operation (AGO) of $X^{(0)}$, whose elements are generated by $I^{k(1)}_{u_n}(i) = \sum_{j=T'-Q}^{i} I^{k\ (0)}_{u_n}(j)$, $i = T'-Q, \cdots, T'-1$. With $X^{(1)}$, the first-order differential equation set is defined as $\frac{dI^{k\ (1)}_{u_n}(i)}{di} + aI^{k(1)}_{u_n}(i) = b$. The least square method is used to find a and b with $\begin{bmatrix} a \\ b \end{bmatrix} = (B^TB)^{-1}B^Tc$, where $B = \begin{bmatrix} -(I^{k(1)}_{u_n}(T'-Q) + I^{k(1)}_{u_n}(T'-Q+1))/2, & 1 \\ \vdots & \\ -(I^{k(1)}_{u_n}(T'-2) + I^{k(1)}_{u_n}(T'-1))/2, & 1 \end{bmatrix}$, and $c = [I^{k(0)}_{u_n}(T'-Q+1)\cdots I^{k(0)}_{u_n}(T'-1)]^T$. Then, the predicted values can be derived as $\hat{I}^{k(1)}_{u_n}(i) = (I^{k(1)}_{u_n}(T'-Q) - b/a)e^{-ai} + b/a$, and $\hat{I}^{k(0)}_{u_n}(T') = \hat{I}^{k(1)}_{u_n}(T') - \hat{I}^{k(1)}_{u_n}(T'-1)$.

Step Two: Assume that the set of the residual error values of $H+1$ moments from time $t - H\tau$ to t is $E = \left\{e^k_{u_n}(t-H\tau), \cdots, e^k_{u_n}(t-\tau), e^k_{u_n}(t)\right\}$. Firstly, divide the elements in E into D states. In this paper, the uniform division way is used to partition the scope of each state. Accordingly,

TABLE III
TRANSITION PROBABILITY TABLE

Initial state	Transition state 1	Transition state 2	$\cdots$	Transition state D
Initial state $d_{t-t_1\tau}$ in time $t-t_1\tau$	$p^{(t_1+1)}_{d_{t-t_1\tau},1}$	$p^{(t_1+1)}_{d_{t-t_1\tau},2}$	$\cdots$	$p^{(t_1+1)}_{d_{t-t_1\tau},D}$
$\cdots$	$\cdots$	$\cdots$	$\cdots$	$\cdots$
Initial state $d_{t-\tau}$ in time $t-\tau$	$p^{(2)}_{d_{t-\tau},1}$	$p^{(2)}_{d_{t-\tau},2}$	$\cdots$	$p^{(2)}_{d_{t-\tau},D}$
Initial state d_t in time t	$p^{(1)}_{d_t,1}$	$p^{(1)}_{d_t,2}$	$\cdots$	$p^{(1)}_{d_t,D}$
The sum of transition probabilities	$\sum_{i=0}^{t_1} p^{(i+1)}_{d_{t-i\tau},1}$	$\sum_{i=0}^{t_1} p^{(i+1)}_{d_{t-i\tau},2}$	$\cdots$	$\sum_{i=0}^{t_1} p^{(i+1)}_{d_{t-i\tau},D}$

the scope of state $d \in \{1, 2, \cdots, D\}$ can be expressed as $(\min(E)+(d-1)\cdot\frac{\max(E)-\min(E)}{D}, \min(E)+d\cdot\frac{\max(E)-\min(E)}{D}]$. Secondly, construct the state transition probability matrix. Let $p^{(q)}_{ij} = \frac{M^{(q)}_{ij}}{M_i}$ stands for the q-step transition probability, where M_i and $M^{(q)}_{ij}$ are the number of state i and the transition sample number from state i to j after the duration of $q\tau$ (q steps). Thus, the q-order transition probability matrix can be constructed as $P^{(q)} = (p^{(q)}_{ij})_{D\times D}$. Thirdly, form transition probability table and calculate the sum of transition probability. Calculate the t_1+1 transition probability matrixes from 1-order to (t_1+1)-order. If the state at time $t-i\tau$, $i \in [0, t_1]$, is $d_{t-i\tau}$, put the $d_{t-i\tau}-th$ row of $(i+1)$-order transition probability matrix into the row, related to time $t-i\tau$, in Table III. Then, the transition probability sum of each transition state is calculated, and find the greatest one to be treated as the most likely state of time $t+\tau$. Finally, assume that the most likely state is d^*, the corresponding most likely residual error can be obtained by

$$\tilde{e}^k_{u_n}(t+\tau) = \min(E) + \left(d^* - \frac{1}{2}\right)\cdot\frac{\max(E)-\min(E)}{D}. \tag{34}$$

APPENDIX B
SOLUTION PROCESS OF (33)

The overall solution process is divided into the suboptimal channel assignment, and the optimal power distribution with a fixed channel assignment, which can be described as:

1. Initialization: Initialize $\mathbf{P}_{unli}$ by equal power distribution, namely, $\bar{p}^k_{n,u_n} = \frac{P^{\max}_{unli}}{N\cdot K}$. Besides, set $\Phi_{u_n} = \varnothing$.

2. Channel assignment:

1) For $\forall u_n \in \Omega$, find an unlicensed channel k^* with the largest reliability utility $UoR^{k^*}_{n,u_n}$ than others in $\Delta_{unli,n}$. Let $\Phi_{u_n} = \Phi_{u_n} \cup \{k^*\}$ and $\Delta_{unli,n} = \Delta_{unli,n} - \{k^*\}$.

2) Repeat

Find the user u_n with the smallest $A_{u_n} = \frac{\sum_{k\in\Phi_{u_n}} B\log_2\left(1+\frac{\bar{p}^k_{n,u_n}\cdot\left|h^k_{n,u_n}\right|^2}{\sum_{m\in\mathbf{N},m\neq n}\bar{p}^k_{m,u_m}\cdot\left|h^k_{m,u_n}\right|^2+I^k_{u_n}}\right)}{R^{req,tot}_{u_n}}$. For found u_n, find k^* with the largest UoR^k_{n,u_n} and let $\Phi_{u_n} = \Phi_{u_n} \cup \{k^*\}$ and $\Delta_{unli,n} = \Delta_{unli,n} - \{k^*\}$.

Until $A_{u_n} \geq 1$ for $\forall u_n \in \Omega$.

3. Power distribution: With the fixed unlicensed channel assignment, the optimization problem (33) can be solved by Lagrangian and KKT condition, by which the optimal power distribution for given Lagrange multipliers can be obtained. And the optimal Lagrange multipliers can be attained by subgradient method.

REFERENCES

[1] CISCO Whitepaper, "CISCO visual networks index: Global mobile data traffic forecast update," CISCO, San Jose, CA, USA, White Paper 2015–2020, Feb. 2016.

[2] R. Zhang, M. Wang, L. X. Cai, Z. Zheng, X. Shen, and L.-L. Xie, "LTE-unlicensed: The future of spectrum aggregation for cellular networks," *IEEE Wireless Commun.*, vol. 22, no. 3, pp. 150–159, Jun. 2015.

[3] M. R. Khawer, J. Tang, and F. Han, "usICIC—A proactive small cell interference mitigation strategy for improving spectral efficiency of LTE networks in the unlicensed spectrum," *IEEE Trans. Wireless Commun.*, vol. 15, no. 3, pp. 2303–2311, Mar. 2016.

[4] Q. Chen, G. Yu, R. Yin, A. Maaref, G. Y. Li, and A. Huang, "Energy efficiency optimization in licensed-assisted access," *IEEE J. Sel. Areas Commun.*, vol. 34, no. 4, pp. 723–734, Apr. 2016.

[5] Z. Pi and F. Khan, "An introduction to millimeter-wave mobile broadband systems," *IEEE Commun. Mag.*, vol. 49, no. 6, pp. 101–107, Jun. 2011.

[6] J. G. Andrews *et al.*, "What will 5G be?" *IEEE J. Sel. Areas Commun.*, vol. 32, no. 6, pp. 1065–1082, Jun. 2014.

[7] A. Al-Dulaimi, S. Al-Rubaye, Q. Ni, and E. Sousa, "5G communications race: Pursuit of more capacity triggers LTE in unlicensed band," *IEEE Veh. Technol. Mag.*, vol. 10, no. 1, pp. 43–51, Mar. 2015.

[8] S. Zhou, T. Zhao, Z. S. Niu, and S. D. Zhou, "Software-defined hyper-cellular architecture for green and elastic wireless access," *IEEE Commun. Mag.*, vol. 54, no. 1, pp. 12–19, Jan. 2016.

[9] R. Wang, H. Hu, and X. Yang, "Potentials and challenges of C-RAN supporting multi-RATs toward 5G mobile networks," *IEEE Access*, vol. 2, pp. 1187–1195, 2014.

[10] Z. Shen, J. G. Andrews, and B. L. Evans, "Adaptive resource allocation in multiuser OFDM systems with proportional rate constraints," *IEEE Trans. Wireless Commun.*, vol. 4, no. 6, pp. 2726–2737, Nov. 2005.

[11] X. Ge, J. Chen, C. X. Wang, J. S. Thompson, and J. Zhang, "5G green cellular networks considering power allocation schemes," *Sci. China Inf. Sci.*, vol. 59, no. 2, pp. 1–14, Feb. 2016.

[12] X. Ma, M. Sheng, J. Li, and Q. Yang, "Concurrent transmission for energy efficiency of user equipment in 5G wireless communication networks," *Sci. China Inf. Sci.*, vol. 59, no. 2, pp. 1–15, Feb. 2016.

[13] F. Haider, C. X. Wang, B. Ai, H. Haas, and E. Hepsaydir, "Spectral/energy efficiency tradeoff of cellular systems with mobile femtocell deployment," *IEEE Trans. Veh. Technol.*, vol. 65, no. 5, pp. 3389–3400, May 2015.

[14] W. Zhang, C. X. Wang, D. Chen, and H. Xiong, "Energy–spectral efficiency tradeoff in cognitive radio networks," *IEEE Trans. Veh. Technol.*, vol. 65, no. 4, pp. 2208–2218, Apr. 2015.

[15] C. Xiong, G. Y. Li, S. Zhang, Y. Chen, and S. Xu, "Energy- and spectral-efficiency tradeoff in downlink OFDMA networks," *IEEE Trans. Wireless Commun.*, vol. 10, no. 11, pp. 3874–3886, Sep. 2011.

[16] J. Akhtman and L. Hanzo, "Power versus bandwidth-efficiency in wireless communications: The economic perspective," in *Proc. VTC-Fall*, Anchorage, AK, USA, Sep. 2009, pp. 1–5.

[17] P. Patcharamaneepakorn *et al.*, "Spectral, energy and economic efficiency of 5G multi-cell massive MIMO systems with generalized spatial modulation," *IEEE Trans. Veh. Technol.*, to be published.

[18] I. Ku, C. X. Wang, and J. Thompson, "Spectral, energy and economic efficiency of relay-aided cellular networks," *IET Commun.*, vol. 7, no. 14, pp. 1476–1486, Sep. 2013.

[19] K. Son, H. Kim, Y. Yi, and B. Krishnamachari, "Base station operation and user association mechanisms for energy-delay tradeoffs in green cellular networks," *IEEE J. Sel. Areas Commun.*, vol. 29, no. 8, pp. 1525–1536, Sep. 2011.

[20] M. Sheng, Y. Z. Li, X. J. Wang, J. D. Li, and Y. Shi, "Energy efficiency and delay tradeoff in device-to-device communications underlaying cellular networks," *IEEE J. Sel. Areas Commun.*, vol. 34, no. 1, pp. 92–106, Aug. 2015.

[21] P. Li, Y. Fang, J. Li, and X. Huang, "Smooth trade-offs between throughput and delay in mobile ad hoc networks," *IEEE Trans. Mobile Comput.*, vol. 11, no. 3, pp. 427–438, Mar. 2012.

[22] M. Assaad, "Reduction of the feedback delay impact on the performance of scheduling in OFDMA systems," in *Proc. IEEE 70th Veh. Technol. Conf. Fall (VTC Fall)*, Anchorage, AK, USA, Sep. 2009, pp. 1–4.

[23] H. Dai, Y. Wang, C. Shi, and W. Zhang, "The evaluation of CQI delay compensation schemes based on Jakes' model and ITU scenarios," in *Proc. IEEE Veh. Technol. Conf. (VTC Fall)*, Sep. 2012, pp. 1–5.
[24] D. Goker, "Robust link adaptation in HSPA evolved," M.S. thesis, Eng., Department Commun. Syst., Roy. Inst. Technol., Stockholm, Sweden, Feb. 2009.
[25] C.-L. I, J. Huang, R. Duan, C. Cui, J. Jiang, and L. Li, "Recent progress on C-RAN centralization and cloudification," *IEEE Access*, vol. 2, pp. 1030–1039, Aug. 2014.
[26] Y. M. Shobowale and K. A. Hamdi, "A unified model for interference analysis in unlicensed frequency bands," *IEEE Trans. Wireless Commun.*, vol. 8, no. 8, pp. 4004–4013, Aug. 2009.
[27] E. Perahia and R. Stacey, *Next Generation Wireless LANs*. Cambridge, U.K.: Cambridge Univ. Press, 2008.
[28] S. Srinivasa and S. A. Jafar, "Cognitive radios for dynamic spectrum access—The throughput potential of cognitive radio: A theoretical perspective," *IEEE Commun. Mag.*, vol. 45, no. 5, pp. 73–79, May 2007.
[29] C. Fan, Z. Jin, W. Tian, and F. Qian, "Grey Markov chain and its application in drift prediction model of FOGs," *J. Syst. Eng. Electron.*, vol. 16, no. 2, pp. 388–393, Jun. 2005.
[30] Y. He and Y. D. Bao, "Grey-Markov forecasting model and its application," *Syst. Eng. Theory Pract.*, vol. 4, pp. 59–63, Jul. 1992.
[31] S. Stotas and A. Nallanathan, "Enhancing the capacity of spectrum sharing cognitive radio networks," *IEEE Trans. Veh. Technol.*, vol. 60, no. 8, pp. 3768–3779, Aug. 2011.
[32] W. Q. Xu, Q. J. Shi, X. Y. Wei, Z. Ma, X. Zhu, and Y. M. Wang, "Distributed optimal rate-reliability-lifetime tradeoff in time-varying wireless sensor networks," *IEEE Trans. Wireless Commun.*, vol. 13, no. 9, pp. 4836–4847, Jul. 2014.
[33] J.-W. Lee, M. Chiang, and A. R. Calderbank, "Price-based distributed algorithms for rate-reliability tradeoff in network utility maximization," *IEEE J. Sel. Areas Commun.*, vol. 24, no. 5, pp. 962–976, May 2006.
[34] H. Song, X. Fang, L. Yan, and Y. Fang, "Control/user plane decoupled architecture utilizing unlicensed bands in LTE systems," *IEEE Wireless Commun.*, to be published.
[35] Q. T. Nguyen-Vuong, N. Agoulmine, E. H. Cherkaoui, and L. Toni, "Multicriteria optimization of access selection to improve the quality of experience in heterogeneous wireless access networks," *IEEE Trans. Veh. Technol.*, vol. 62, no. 4, pp. 1785–1800, Dec. 2012.
[36] Y. Ma and D. I. Kim, "Rate-maximization scheduling schemes for uplink OFDMA," *IEEE Trans. Wireless Commun.*, vol. 8, no. 6, pp. 3193–3205, Jun. 2009.
[37] D. P. Palomar and M. Chiang, "A tutorial on decomposition methods for network utility maximization," *IEEE J. Sel. Areas Commun.*, vol. 24, no. 8, pp. 1439–1451, Aug. 2006.
[38] L. Pierucci, "The quality of experience perspective toward 5G technology," *IEEE Wireless Commun.*, vol. 22, no. 4, pp. 10–16, Aug. 2015.
[39] P. Kyösti *et al.*, "WINNER II channel models," D1.1.2, V1.2, Sep. 2007.
[40] ITU-R Report, "Guideline for evaluation of radio interface technologies for IMT-advanced," Radiocommun. Bureau, Geveva, Switzerland, Tech. Rep. ITU-R M.2135-1, Dec. 2009.

Hao Song (S'14) received the B.E. degree in electrical information engineering from Zhengzhou University, Zhengzhou, China, in 2011. He is currently pursuing the Ph.D. degree with the Key Laboratory of Information Coding and Transmission, School of Information Science and Technology, Southwest Jiaotong University, Chengdu, China. His research interests focus on mobile network optimization, unlicensed spectra cognitive systems, next generation mobile networks for high-speed railway, and 5G mobile networks.

Xuming Fang (SM'16) received the B.E. degree in electrical engineering, the M.E. degree in computer engineering, and the Ph.D. degree in communication engineering from Southwest Jiaotong University, Chengdu, China, in 1984, 1989, and 1999, respectively. In 1984, he was a faculty member with the Department of Electrical Engineering, Tongji University, Shanghai, China. He joined the Key Laboratory of Information Coding and Transmission, School of Information Science and Technology, Southwest Jiaotong University, where he has been a Professor since 2001 and the Chair of the Department of Communication Engineering since 2006. He held visiting positions with the Institute of Railway Technology, Technical University Berlin, Berlin, Germany, in 1998 and 1999, and with the Center for Advanced Telecommunication Systems and Services, The University of Texas at Dallas, Richardson, TX, USA, in 2000 and 2001. He has to his credit around 200 high-quality research papers in journals and conference publications. He has authored or co-authored five books or textbooks. His research interests include wireless broadband access control, radio resource management, multihop relay networks, and broadband wireless access for high speed railways. He is an Editor of the IEEE TRANSACTIONS ON VEHICULAR TECHNOLOGY, the *Journal of Electronics and Information*, and the Chair of the IEEE Vehicular Technology Society Chengdu Chapter.

Cheng-Xiang Wang (S'01–M'05–SM'08–F'17) received the B.Sc. and M.Eng. degrees in communication and information systems from Shandong University, China, in 1997 and 2000, respectively, and the Ph.D. degree in wireless communications from Aalborg University, Denmark, in 2004.

He has been with Heriot-Watt University, Edinburgh, U.K., since 2005, and was promoted to Professor in 2011. He is also an Honorary Fellow of The University of Edinburgh, U.K., and a Chair/Guest Professor at Shandong University and Southeast University, China. He was a Research Fellow with the University of Agder, Grimstad, Norway, from 2001 to 2005, a Visiting Researcher with Siemens AG Mobile Phones, Munich, Germany, in 2004, and a Research Assistant with Hamburg University of Technology, Hamburg, Germany, from 2000 to 2001. He has authored one book, one book chapter, and about 260 papers in refereed journals and conference proceedings. His current research interests include wireless channel modeling and 5G wireless communication networks, including green communications, cognitive radio networks, high mobility communication networks, massive MIMO, millimeter wave communications, and visible light communications.

Dr. Wang served or is currently serving as an Editor for 12 international journals, including the IEEE TRANSACTIONS ON VEHICULAR TECHNOLOGY since 2011, the IEEE TRANSACTIONS ON COMMUNICATIONS since 2015, and the IEEE TRANSACTIONS ON WIRELESS COMMUNICATIONS from 2007 to 2009. He was the leading Guest Editor of the IEEE JOURNAL ON SELECTED AREAS IN COMMUNICATIONS Special Issue on Vehicular Communications and Networks. He served or is serving as a TPC member, TPC chair, and general chair for over 80 international conferences. He received nine Best Paper Awards from the IEEE Globecom 2010, the IEEE ICCT 2011, the ITST 2012, the IEEE VTC 2013-Spring, the IWCMC 2015, the IWCMC 2016, the IEEE/CIC ICCC 2016, and the WPMC 2016. He is a fellow of the IET and HEA, and a member of the EPSRC Peer Review College.